LITERATURE REVIEW – ALLOY TI6-4 ELABORATED BY POWDER BED FUSION TECHNOLOGIES: HEAT TREATMENTS

Abstract

Microstructure of alloy Ti6-4 elaborated by Powder Bed Fusion technologies presents differences to ones traditionally characterized after conventional elaboration processes. One of the particularity is the high cooling rates experienced by the material leading to out of equilibrium microstructures. This literature review aims to report the different heat treatments nowadays performed or studied on alloy Ti6-4 elaborated by these additive manufacturing processes.

DATE : 23/11/2018

RÉFÉRENCE : LIV-M-031-L6-490

Author(s)	*Function(s) & name(s)*	*Research Engineer*	*Jonathan HUGUES*
Checker(s)	*Function(s) & name(s)*	*Project Manager*	*Céline LARIGNON*
		Quality Manager	*Stéphane BENAZET*
Approver	*Function & name*	*R&T Manager*	*Simon PERUSIN*

Table of Contents

Revision Table

Issue	Date	modified §	Evolution summary	Modified by
1	23/11/18	All	Creation	All

Table of figures

1 General introduction

1.1 Heat treatments

Heat treatment is an important step in producing a part. Several steps can be necessary to reach the desired microstructure guaranteeing the mechanical properties. Behind the designation heat treatment, several steps can be needed to shape the microstructure, depending on the alloy. In the case of AnDDurO project, three alloys with different heat treatment routines are used. On the contrary of alloy Ti64, alloys AS7G06 and 718 are precipitation hardened alloys, meaning that their mechanical properties can be tailored by the management of precipitates.

In general, different types of heat treatment with their own objective can be used. A non-explicit list is proposed here.

- Homogenisation heat treatment. The goal of this step is to reduce the chemical heterogeneity inside a semi product or a part, by heat treating at high temperatures to allow elements diffusion on large distance.
- Solution treatment. During this treatment, one or several phases are dissolved into the matrix to obtain a homogeneous solid solution.
- Recrystallization annealing. During this treatment, nucleation of new grains is occurring leading to a refinement of the grain size.
- Cooling. After these different steps, the part is generally cooled down. Depending on the nature of the alloy, the cooling rate can be very low or very fast. In this case, the goal of the quench is either to allow the formation of a metastable phase, for example martensite in the case of steels, or to freeze the microstructure, for example keeping the supersaturation of an element in the matrix.
- Stress relieving. The main objective of this step is to decrease the intensity of the thermal stresses present inside the part. To complete this objective, a sufficiently high temperature is applied to promote the motion of the dislocations. For precipitation hardened alloys, the applied temperature must be sufficiently high to dissolve the hardening phases, favouring the dislocations movements.
- Tempering. During tempering the goal is to precipitate phase(s) which will lead to an important change of mechanical properties, either softening or hardening.

To determine thermal treatments routes, Temperature – Time – Transformation (TTT) and/or Continuous Cooling Transformation (CCT) diagrams are very useful. They bring data on the precipitation/dissolution temperature – time domain of the different phases and their formation during cooling, respectively. A precise knowledge of these diagrams allow the user to adjust the heat treatment sequence to its needs. The building of these diagrams is a long and meticulous work to determine the precipitation domain of each phases. However, these data are essential to manage the elaboration of thermal routine for heat treatment.

1.2 Hot Isostatic Pressing

In addition to these basic heat treatments, an additional type of procedure can be used when closure of pores are needed. In this case, in addition to the application of high temperature, a high gas pressure is applied to the workload. The process is called Hot Isostatic Pressing, HIP. The combination of these two solicitations lead to a decrease of the temperature needed in case of sintering alone and a lower pressure in case of only compaction. Mechanisms implied during HIP will be detailed in the following paragraph, based on a detailed review written by Atkinson [1].

Before explaining mechanisms occurring during HIP, it is interesting to focus on sintering. This mechanism is based on the diffusion of matter. Usually, the temperature needed to start the sintering is set around 0.7 time melting point of the material. As explained by Atkinson, the driving force is the reduction of the surface area associated with pores. Regions of high disorder, that is to say, related to the presence of

dislocations, grain boundaries and pores, are regions of high energy. The goal of sintering is to lower the overall energy of the material by eliminating all these defects. The lowest energy system, upon which the system tries to tend, is a single crystal with no defects. The driving force to eliminate small pores is greater than the one for large pores. Atkinson estimated that the driving for the closure of a 1 µm pore is 4 MPa compare to the 4 x 10^{-3} MPa needed for a 1 mm pore. Nevertheless, at the end of the sintering process, large pores are remaining. The reason of this is linked with the nature of the pores. When pores are full of gas, the internal pressure will tend to oppose to the driving force of shrinkage. As the shrinkage is going on, the pressure will increase. Then, the gas will tend to dissolve into the matrix and to diffuse to a region of lower pressure, such as large pores or surface. Therefore, large pores are remaining and growing on the contrary of small pores. Moreover, irregular pores will tend to spheroïdize, because of the difference of matter diffusion between concave regions with small radius and convex surfaces. But, this tendency is counterbalanced by the different interfacial energies of the different grains where pores are located. In his review, Atkinson exposes the different mechanisms of matter transportation. These will not be detailed in this document.

During Hot Isostatic Pressing, gas is used to apply a mechanical loading on the workload. As Atkinson explained *"each gas atom is acting as an individual "hot forge". Under particular processing conditions, the gas atoms may be moving at a velocity of around 900 m.s^{-1}, and approximately 10^{30} collisions events are occurring per square meter per second."* Usually a pressure of 100 MPa is set into the vessel. This pressure needs to be compared to the 4 MPa required to close a pore of 1 mm in diameter. In consequence, gases in pores are dissolving into the matrix on the contrary to argon used for pressurization in hipping. Moreover, the solubility of gases increases with the increasing pressure within the pore. However, the discussion led by Atkinson is particularly focusing on casted material, where argon is rarely trapped during solidification, which is not the case in additive manufacturing.

As the yield strength is generally decreasing with the increase of temperature, the material exhibits a yield strength lower than the pressure set during HIP cycle. So, plastic flow can occur at a microscopic scale. Shearing of particles and creep phenomena are happening during the thermal cycle. Atkinson clarifies that different mechanism of creep can occur. It is usual that oxide is still present on the surface of a pores. Particles shearing can break up the oxide layer, leading to the formation of a new surface and enhancing surface diffusion rates. But, on the contrary, some oxide particles can still be present after HIP, degrading mechanical properties of the part. Finally, at the end of hipping process, when last pores are isolated, the pressure is not only pushing interfaces between each other. As the temperature is high, diffusion of elements is occurring leading to the bonding of the different side of the pores. However, as for conventional heat treatment, use of high temperatures can lead to several issues such as chemical segregation or excessive grain growth.

Nonetheless, the application of a high pressure may change the transformation temperature of an alloy. For example, Atkinson highlights the fact that the melting point is increasing if the material shrinks, which is the case for most of them. But, this effect is quite reduced, about a few degrees Celsius. Moreover, Lyubov [2] explained that the application of a high pressure can lead to either an increase or decrease of the kinetic of phase transformation. The author highlighted two major causes explaining these modifications. First, the thermodynamic driving force is influenced by the pressure, related to the change of density of the material during the phase transformation. Indeed, pressure changes the solute equilibrium concentration, affecting the kinetics of phase transformation. Second, the pressure is affecting the diffusion of solute elements.

More recently, some studies has focused on the effect of the pressure on phase transformation. These studies are motivated by the fact that modern HIP vessels possess the capability of reaching high cooling rates, opening the possibility of using HIP vessel not only for the consolidation of parts, but as a mean to perform heat treatment. An example of using HIP for performing heat treatment by using high cooling rates is presented by Mashl [3] on steel. By comparing the results of samples submitted to the same heat treatment but performed with an oil, a water and a HIP quench, the author revealed that using the HIP quench leads to hardness values slightly lower to oil quench but higher than water quench. Even if the cooling rate measured is in the range of 5-10 °C/s, compared to several tens of °C/s in the case of oil quench, the microstructure is a mix of what is observed after oil and water quench. The reason for this has to be searched

on the decomposition of the austenite into ferrite and cementite. As reported in Figure 1, the application of an isostatic pressure leads to the shift of precipitation nose to the lower temperatures and higher time. Moreover, Mashl indicates that the obtained microstructure is finer than the one observed after treatment under atmospheric pressure. Other studies reveal the same effect of pressure on the microstructure and resultant mechanical properties on steel [4] [5].

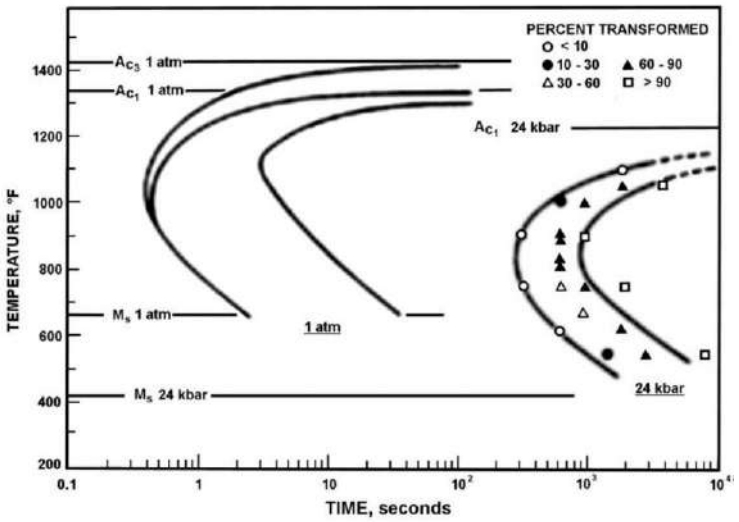

Figure 1: TTT diagram for 1040 steel at atmospheric pressure and 24 kbar (2400 MPa) [3]

Finally, Atkinson [1] highlights the fact that porosity shall not remain stable during heat treatment without pressure after HIP. As already mentioned, pores full of gases can collapse during HIP, by the dissolution of gases into matrix. Nevertheless, during subsequent heat treatment, gas contained in the matrix tends to reach an equilibrium pressure dependent on the surface tension. Thus, swelling of pores can be observed, *i.e.* the reappearance of pores. This phenomenon will be shown in parts dedicated to alloy Ti6-4, as it has been experimentally observed.

1.3 Goal of the document

Microstructures of alloys Ti6-4 and 718 elaborated by Powder Bed Fusion processes, LBM and EBM, are exposed in the IRT document LIV-M-031-L1-409. Because of the specific features of processes, microstructure are quite different from the ones obtained from conventional manufacturing processes. In sections dedicated to each alloy, a brief summary of the microstructure and the resulting problematics will be exposed. However, as microstructures are different in their as-built conditions, their responses to heat treatment must be too. Moreover, some of the microstructures present some elements that need to be erased in order to be used for structural parts.

This document will present heat treatments commonly used on both alloys at the moment of the writing of the document. Microstructure evolution and the influence on mechanical properties will be exposed.

2 Heat treatments performed on alloy Ti6-4 processed by PBF

2.1 Alloy Ti6-4 and LBM

The use of alloy Ti6-4 is spread into different industrial sector. This is due to a good knowledge of its metallurgy and especially the phase transformation of the alloy. As for steels, alloy Ti6-4 microstructure is dependent on the cooling after high temperature treatment. In consequence, Continuous Cooling Transformation, CCT, diagrams are usually used to set the procedure. An example is presented in Figure 2.

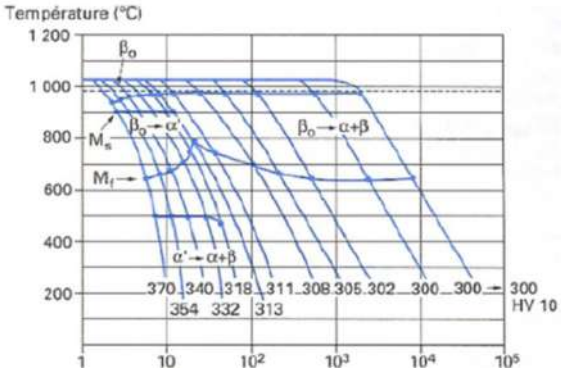

Figure 2: Example of CCT diagram after solution treatment at 1025°C

A schematic diagram is proposed in Figure 3. From this schematic view, it can be seen that martensite, α' phase, can be formed for high cooling rate, superior to 410°C/s according to Ahmed [6], Figure 3. For lower cooling rate, the microstructure is composed of α and β phases. The martensite start transformation point Ms temperature is increasing with the decreasing of cooling rate.

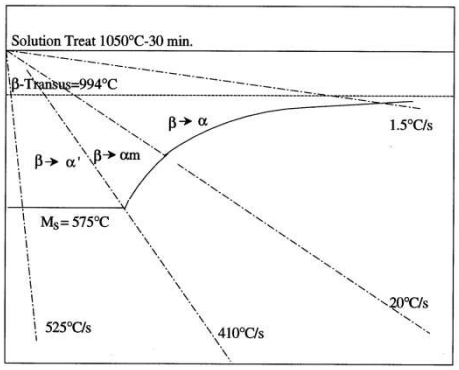

Figure 3: Schematic CCT diagram after solution treatment at 1050°C [6]

Because of high cooling rates and directional thermal gradient, the microstructure of alloy Ti6-4 processed by LBM is composed of a very fine martensite laths and columnar prior β grains orientated according to the building direction. It is reminded here that martensite is an out of equilibrium phase obtained after a rapid cooling from the β domain. This microstructure leads to anisotropic mechanical properties, dependent on the solicitation axis. More detailed on the microstructure of alloy Ti6-4 processed by Laser Beam Melting, LBM, is presented in LIV-M-031-L1-409.

Therefore, as martensite is a hard but brittle phase, its management is of great importance when dealing with structural parts, where ductility and toughness are often required. Moreover, even if a columnar structure can be beneficial for some applications, for most cases, an isotropic material is preferred. Nevertheless, because of high cooling rates, martensite laths are small, participating to the high strength of the alloy. A small microstructure can be of great interest for industrial applications, as it generally leads to high strength material, as outlined by the Hall-Petch relationship.

2.1.1 Evolution of microstructure

Several strategies can be led for performing heat treatments on alloy Ti6-4. A decomposition can be made depending on the maximum temperature reached. If this one is inferior to the β transus transformation point, about 990°C in the case of alloy Ti6-4, the heat treatment can be qualified as sub-transus. On the contrary, when the β transus transformation point is exceeded, the heat treatment can be qualified as super-transus. This decomposition will be used for this literature review.

(a) Sub-transus heat treatment

This heat treatment strategy is led at moderate temperatures. First heat treatments considered here are the ones happening at temperature lower than 800°C. Several microstructure obtained after different heat treatments are presented hereafter.

In Figure 4, two heat treatments have been performed at 600°C and 700°C. The microstructure observed after heat treatment at the lowest temperature does not show great difference with an as-built microstructure. Needles are still observed. At 700°C, the needle-like microstructure is observed, but, the presence of α phase at the grain boundaries of the prior β grains have to be outlined. X-Ray Diffraction XRD analysis have been performed on these samples. Results are presented in Figure 5.

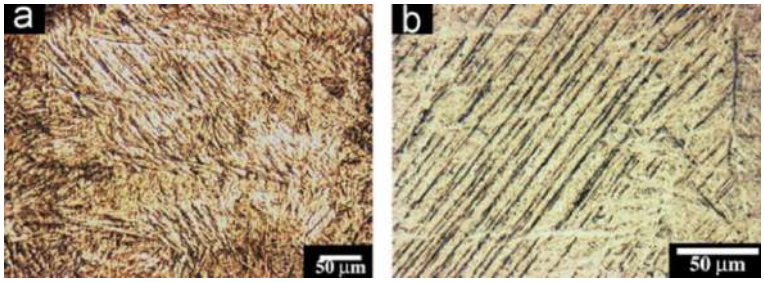

Figure 4: Microstructure of alloy Ti6-4 produced by LBM after heat treatment during 2 hours at a) 600°C and b) 700°C followed by a furnace cooling [7]

When comparing the diagram obtained for the as-fabricated to the other ones, slight differences appear. First, peaks corresponding to α phase are shifted to the lower 2θ angles. As explained by Qiu [7], this is related to the transformation of α' martensite to α phase. Nevertheless, this decomposition is only partial, as microstructure observations show.

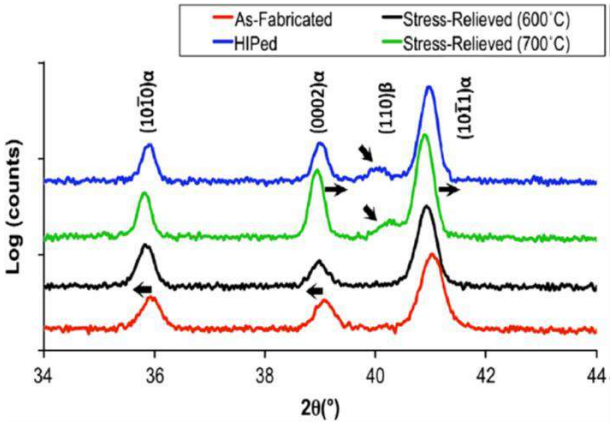

Figure 5: XRD analysis on as-built and heat treated samples [7]

Then, for heat treatment at 700°C, another peak is appearing at 2θ equals 40°. This peak is characteristic of the (110) plan of the β phase. This indicates that at this temperature, the formation of this phase is starting. In this study, Qiu [7] called this treatment stress relieving. Indeed, the microstructure evolution is quite low and the Full-Width Half-Maximum (FWHM) of the different peaks is decreasing,

revealing the decrease of the residual stresses. Vilaro [8] specified that a heat treatment of 2 hours at 730°C is sufficient to completely relieve the residual stresses.

The result of this heat treatment on the microstructure is observed on Figure 6. The microstructure is composed of α lamellae. The presence of α' martensite is observed too. Moreover, some light zones appeared, sign of the presence of β phase. Moreover, Vilaro outlined the fact that the prior β grains do not evolve after this type of treatment.

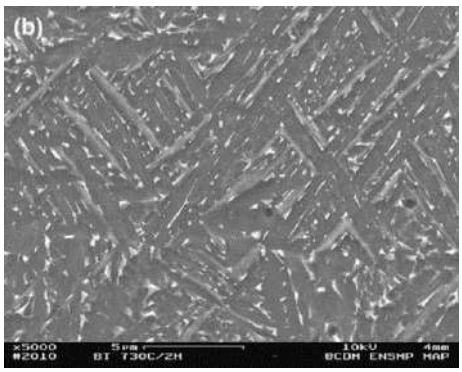

Figure 6: Microstructure of alloy Ti6-4 produced by LBM after heat treatment during 2 hours at 730°C followed by a furnace cooling [8]

The presence of β phase is highlighted after a heat treatment at 780°C for two hours, Figure 7. However, the author did not reveal the presence of α' martensite, suggesting that its decomposition in α phase is completed. In his paper, Vilaro [8] explained that the decomposition of α' martensite is completed after heat treatment at 800°C for 2 hours. These data are extracted from experiments performed on conventionally manufactured alloy Ti6-4. Considering the size of the martensite and a different chemical segregation of elements, it is reasonable to think that a complete decomposition can happen at a lower temperature.

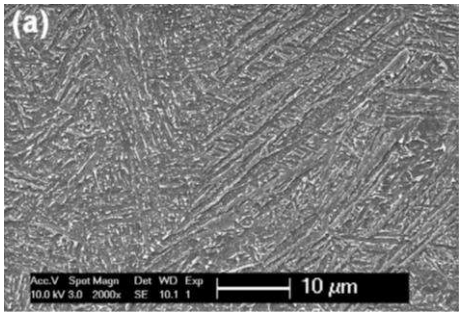

Figure 7: Microstructure of alloy Ti6-4 produced by LBM after heat treatment during 2 hours at 780°C followed by a furnace cooling [9]

The microstructure after a heat treatment at 843°C for 2 hours is presented in Figure 8. By comparing it with the one presented in Figure 7, an increase of the lamellae size as well as the quantity of β phase is observed. This tendency is not surprising, considering the fact that the temperature is getting closer to the β transus.

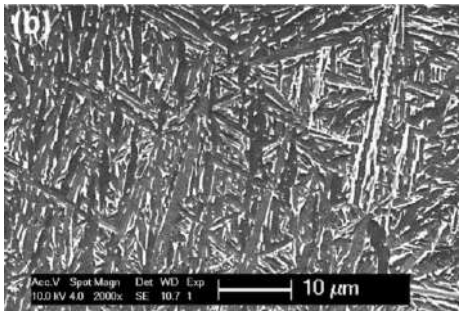

Figure 8 : Microstructure of alloy Ti6-4 produced by LBM after heat treatment during 2 hours at 843°C followed by a furnace cooling [9]

An example of microstructure after heat treatment 900°C for 2 hours followed by an annealing at 700°C for 1 hour is presented in Figure 9. The microstructure is composed of α lamellae in a β matrix. The increase of the temperature leads to the coarsening of the lamellae, with a width of about 3 µm.

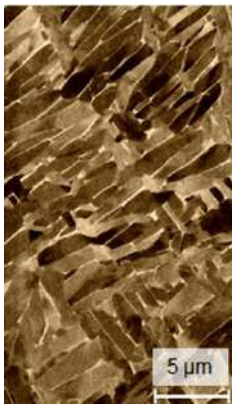

Figure 9: Microstructure of alloy Ti6-4 produced by LBM after heat treatment during 2 hours at 900°C followed by an annealing at 700°C during 1 hour [9]

The evolution of the quantity of the phase during heat treatment has been studied for alloy Ti6-4. We can cite here the work performed by Pederson [10] using High Temperature XRD on a duplex alloy Ti6-4. Results are presented in Figure 10.

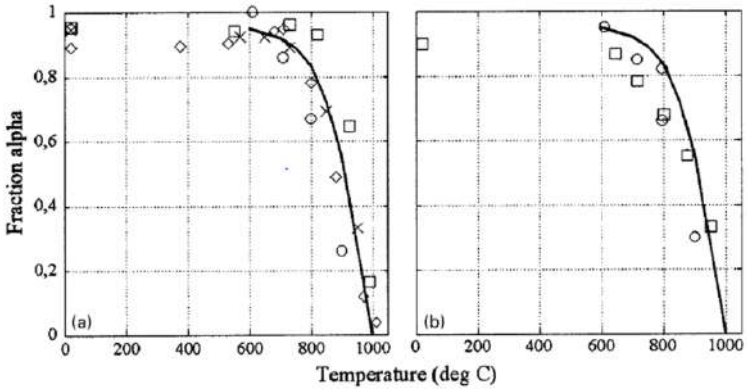

Figure 10: Evolution of the fraction of α phase during a) heating and b) cooling [10]

As we can see on the diagram corresponding to heating, the significant evolution of α phase content starts from about 700°C. From this temperature, the evolution of fraction of α phase is quickly evolving with the temperature. These data are in accordance with the fact exposed earlier in the document that all the martensite is decomposed in α phase after heat treatment of 2 hours at 800°C. After this treatment, β phase fraction is about 15%. From this temperature, we can consider that the alloy is in the (α+β) domain. An example of heat treatment performed at higher temperature is presented in Figure 11.

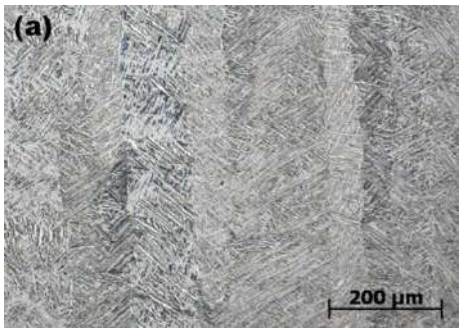

Figure 11: Microstructure of alloy Ti6-4 produced by LBM after heat treatment during 1 hour at 940°C followed by 2 hours at 650°C [9]

In this case, the alloy has been submitted to a tempering after the solution heat treatment. Nevertheless, the microstructure is different from what is observed after manufacturing. Prior β columnar grains are still observed. The temperature is not high enough to destabilize them. But, the microstructure is coarser in this case.

Until now, the increase of temperature has just been discussed. Two other parameters need to be discussed, the cooling rate and the duration of the heat treatment. Vrancken [9] reported that the effect of residence time is limited for heat treatment below the β transus. For example, a heat treatment at 940°C for 2 and 20 hours, the lamellae width is about 2.2 µm and 2.8 µm respectively. About the cooling rate, its effect is insignificant for low temperature, as the fraction of α phase is quite large. But, as the temperature is closer to β transus, the slower the cooling rate, the bigger the lamellae. Vilaro reported that a water quench performed after a heat treatment of 1 hour at 950°C lead to the a small amount of α' phase.

(b) Super-transus heat treatment

In the case of super-transus heat treatment, the maximum temperature reached is above the β transus, *i.e.* 990°C. Thus, during the heat treatment, the microstructure is fully transformed into β phase. This will largely affects the morphology of the microstructure. An example is provided in Figure 12.

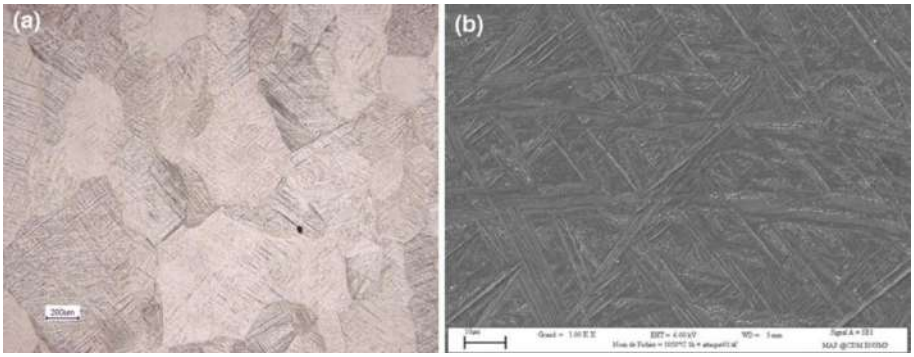

Figure 12: Microstructure of alloy Ti6-4 produced by LBM after heat treatment during 1 hour at 1050°C followed by a water quench [8]

The morphology of the prior β grains is completely different. The columnar grains observed after manufacturing are replaced by large equiaxed grains. Vilaro [8] and Vrancken [9] explained that the width of prior β grains is increasing leading to millimetres grains.

Contrary to sub-transus treatment, the cooling rate and the time spent at high temperature have significant effect on the microstructure. In the case of Figure 12, the super-transus treatment is followed by a water quench. As suggested by the CCT diagram, the water quench leads to the formation of a fresh α' martensite. Nevertheless, the cooling rate is lower than the one happening during LBM process, about 100 times. Consequently, the martensite laths are about 1 µm width, to be compared with the few hundreds of

nanometres after LBM. For cooling rates not leading to the formation of martensite, the quicker the cooling rate, the smaller the size of the lamellae and colony. The cooling rate will determine the morphology of the microstructure, either Widmanstätten type for high cooling rate or in colonies for lower cooling rate.

Vrancken performed a heat treatment at 1040°C for 2 and 20 hours. Resultant microstructures are shown in Figure 13. The comparison of the two microstructures demonstrates that an increase of the residence time at high temperature leads to an increase of size of the lamellae and of the colonies. The presence of α phase at the prior β grains boundaries have to be outlined in both cases.

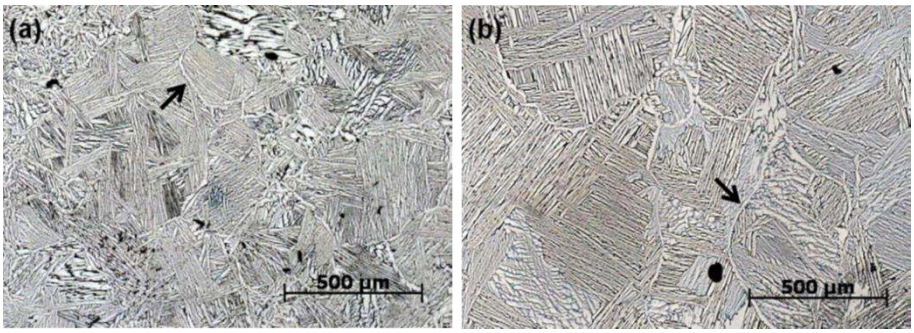

Figure 13: Microstructure of alloy Ti6-4 produced by LBM after heat treatment at a) 1020°C during 2 hours and b) 1040°C during 4 hours followed by a furnace cooling [8]

Solution treatment performed at temperature higher than the β transus is generally followed by an annealing treatment at lower temperature. Vilaro [8] summarised the evolution of hardness and microstructure during annealing at different temperature and cooling rates after a solution treatment at 1050°C for 1 hour and a water quench, Figure 14.

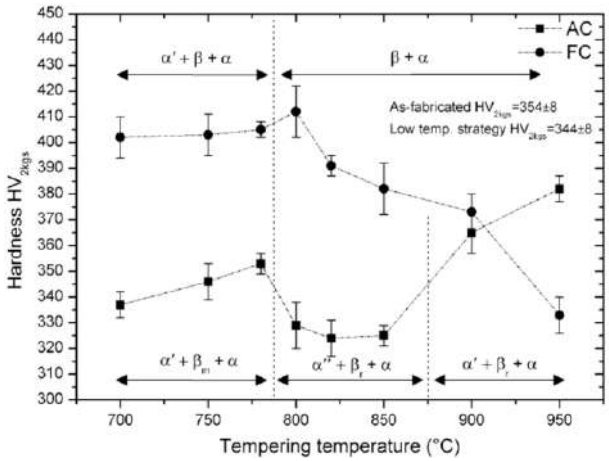

Figure 14: Evolution of hardness and microstructure for annealing treatment performed after solution treatment at 1050°C for 1 hour and water quench [8]

As mentioned in the part dedicated to the sub-transus treatments, the presence of α' martensite due to the quench of the alloy is observed for heat treatment until 780°C. However, microstructure evolution between the two cooling conditions are different. Furnace cooling leads to a slow cooling, meaning that the alloy tends to reach its equilibrium state. This leads to the formation of greater amount of β phase compared to air cooling and more decomposition of α' into α. For temperature higher than 780°C, the microstructure is only composed of α and β phase, the increase of the temperature leading to an increase of the lamellae size. The quicker cooling due to air cooling makes possible to maintain some high temperature β phase stable at room temperature, designated β_m in Figure 14. This is observed until 780°C. For higher temperatures, α'' phase can form. When the temperature reaches 870°C, fresh martensite can be formed, because of the cooling rate sufficient to transform β phase.

(c) Hot Isostatic Pressure

The aim of the HIP heat treatment is to close most of the pores than can be present in additively manufactured parts. However, HIP is used in powder metallurgy to produce parts directly from powder. Nowadays, HIP conditions applied to alloy Ti6-4 are 920°C – 1000 bar – 2 hours. No explicit study on the effect of the HIP conditions is known from the writer in the case of LBM parts. Nevertheless, Xu [11] reported the evolution of the density of the part, tensile mechanical properties and impact toughness, Figure 15.

HIP Conditions	ρ (%)	0.2% YS (MPa)	UTS (MPa)	El. (%)	R.A. (%)	A (kJ/m^2)
800 °C/40 MPa/3 h	97.02	840	905	7.5	10.2	112
800 °C/90 MPa/3 h	99.03	931	981	13.8	43.3	460
800 °C/120 MPa/3 h	99.23	932	980	14.8	47.8	447
910 °C/120 MPa/3 h	99.71	845	930	18.5	48.3	550
940 °C/40 MPa/3 h	98.83	845	917	16.7	46.3	562
940 °C/90 MPa/3 h	99.01	851	922	16.4	47.5	545

Notes: YS, UTS, R.A. and El. are abbreviations of yield strength, ultimate tensile strength, reduction of area and elongation, respectively (same as below).

Figure 15: Evolution of density and mechanical properties depending of HIP conditions [11]

From these data, it can been seen that the best compromise between density, tensile strengths, ductility and impact toughness is reached for HIP performed at 910°C – 1200 bar – 3 hours, which are close to the conditions used on LBM parts.

An example of microstructure of LBM alloy Ti6-4 after HIP treatment at 920°C under 1000 bar during 2 hours is presented in Figure 16.

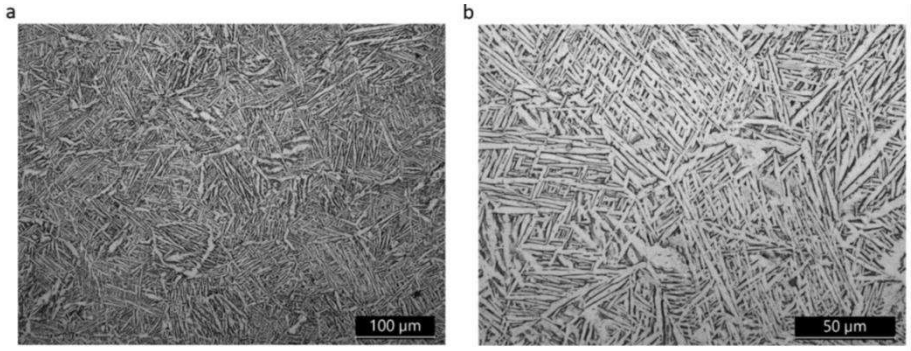

Figure 16 : Microstructure of LBM alloy Ti6-4 after HIP treatment at 920°C – 1000 bar – 2 hours [12]

After HIP, the microstructure is composed of α lamellae surrounded by β phase. Lamellae size is about 3 µm, which is similar to their size obtained after heat treatment at 900°C. Prior columnar β grains are not observed, the microstructure is composed of equiaxed grains.

Effect of HIP on the presence of pores is depicted in Figure 17. The porosity is largely reduced after HIP treatment. Some pores remain, as explained earlier in the document.

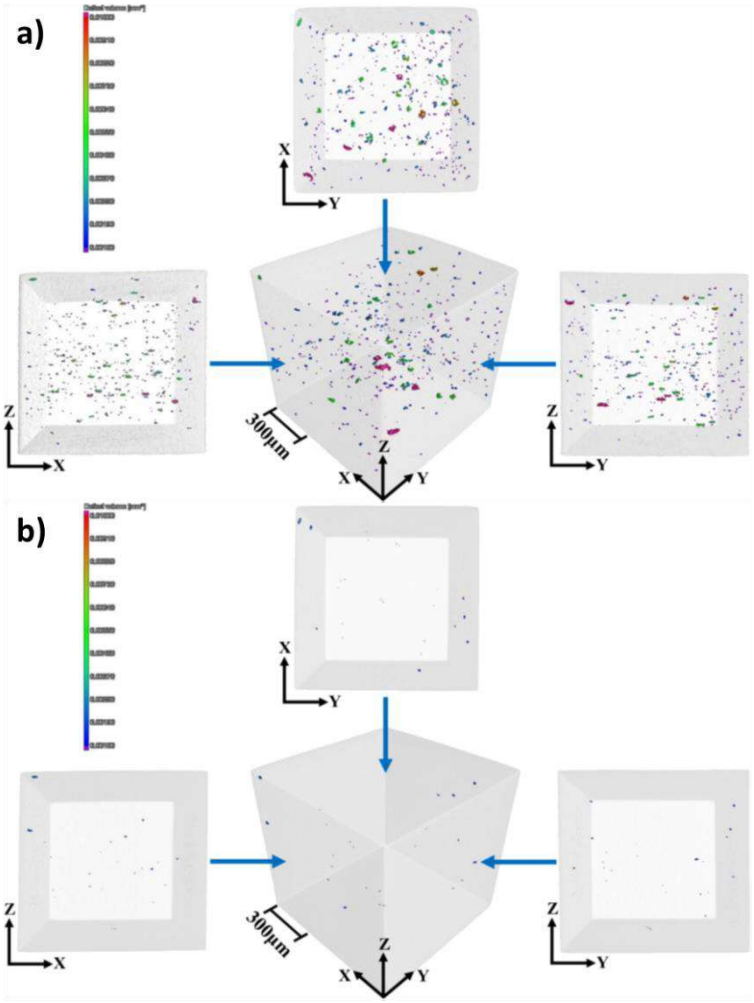

Figure 17: X-Ray CT performed on sample a) in as-built conditions and b) after HIP [13]

2.1.2 Evolution of mechanical properties

Comparison of data between different papers is difficult when considering mechanical properties. Machines and process parameters are always differents leading to a different material. The goal is to show the qualitative influence of heat treatments on mechanical properties, after tensile and fatigue tests.

An example of evolution of tensile behaviour with different heat treatments is reported in Figure 18. These results are compared to wrought alloy Ti6-4.

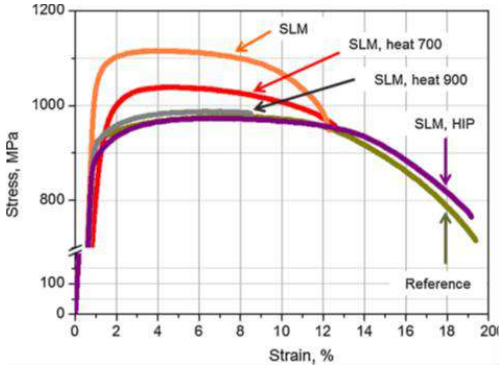

Figure 18: Evolution of tensile behaviour for alloy Ti6-4 submitted to different heat treatments [14]

Fracture surfaces are presented in Figure 19.

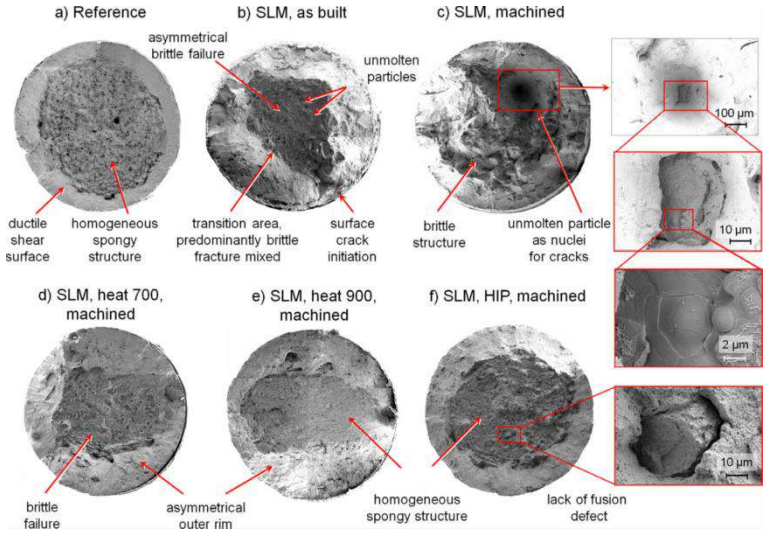

Figure 19: Fracture surface of the different samples tested in Figure 18 [14]

As built LBM samples present high tensile strengths but with a low ductility, because of the presence of martensite. This leads to a brittle behaviour of the fracture. With a heat treatment of two hours at 700°C, as the martensite is partially decomposed into α phase, tensile strengths are lower, of about 100 MPa. The elongation to fracture remains unchanged. The alloy remains brittle, as suggested in Figure 19.

After heat treatment at 900°C, because of the disappearance of martensite and the coarsening of the microstructure, tensile strengths continue to decrease, being comparable to the ones obtained for wrought alloy Ti6-4. Nevertheless, the elongation to fracture remains low, about 9%, with a quite important dispersion, results being in the range of 7.4 to 12.5. The presence of pores may explain these results, as illustrated in Figure 19. After HIP, tensile behaviour is equivalent to the one measured for wrought material. Fracture surface is equivalent to the one of wrought alloy. Nevertheless, some lack of fusion defects are still observed.

Vrancken [9] reported the results of tensile tests after different heat treatments, Figure 20. As in the previous study, as the maximum temperature reached increases, the yield stress decreases. The coarsening of the microstructure and the transformation of martensite into α phase explain these results. On the contrary, the fracture strain increases with the maximum temperature. Nevertheless, it remains quite low, with a maximum of 13 %.

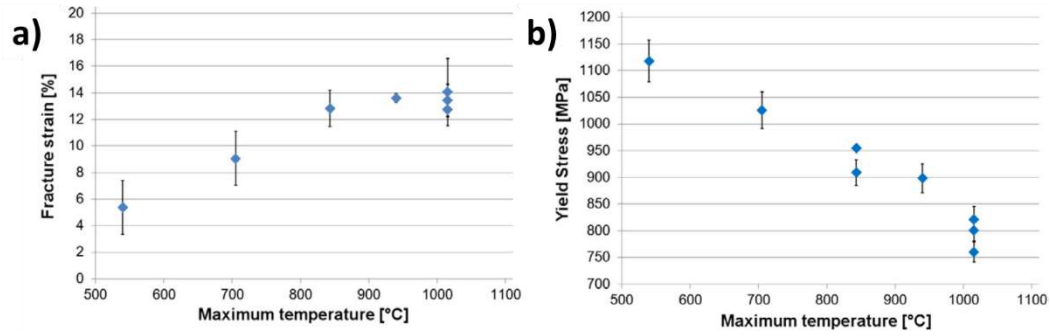

Figure 20: Evolution of fracture strain and Yield Stresses as a function of the maximum temperature reached during the heat treatment [9]

The fatigue behaviour has been investigated by Kasperovich [14] too. The results are presented in Figure 21.

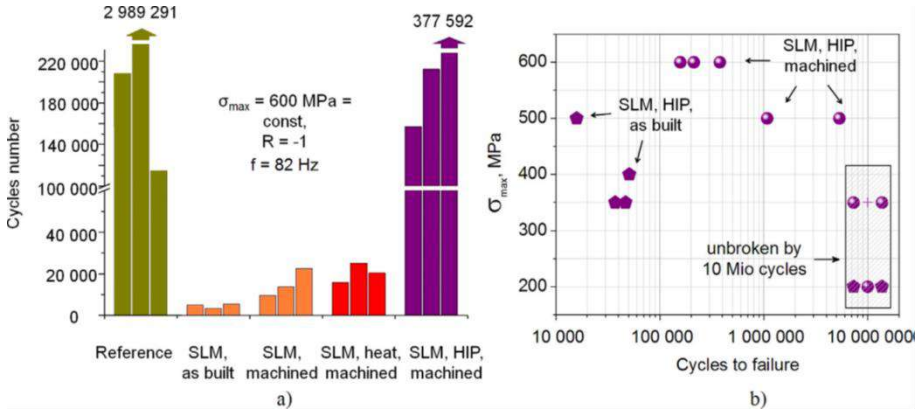

Figure 21: Fatigue behaviour of alloy Ti64 in different metallurgical states [14]

In as-built conditions, machined or not, and after heat treatment at 700°C, the number of cycles to failure is low, especially when comparing to the reference which is a wrought alloy. Fracture surfaces of these samples present a brittle failure mode. For samples not machined, cracks originated from the surface are leading to the premature failure of the alloy. After a HIP treatment, the fatigue behaviour is comparable to the one observed for the reference material. The effect of defects on specimen failure is explaining this tendency, as we can see in Figure 22, as the fracture surface is similar to the one obtained for a wrought alloy Ti64. In Figure 21 b), the effect of the surface roughness is investigated on HIPed specimens. As expected, unmachined specimens possess a lower fatigue behaviour. Cracks present at the surface of the specimens induce premature failure.

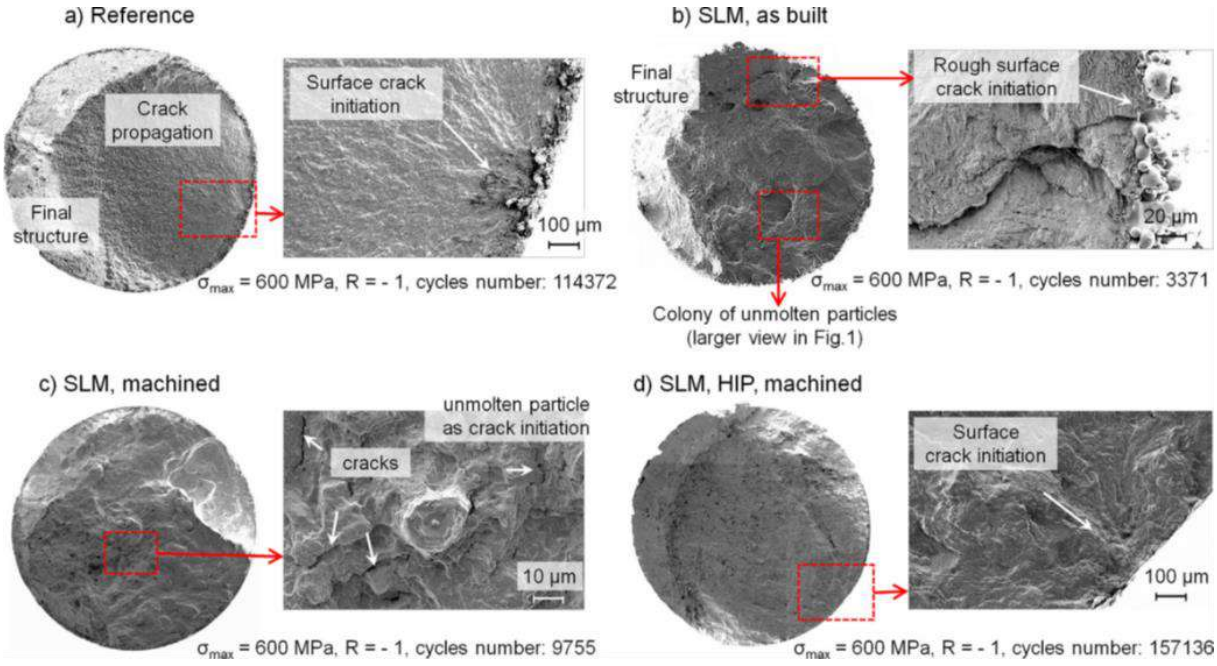

Figure 22: Fracture surface of specimens after fatigue tests [14]

Chastand [15] performed fatigue tests on specimens after stress relieving heat treatment at 650°C for 4 hours and HIP at 920°C – 1000 bars – 2 hours, Figure 23.

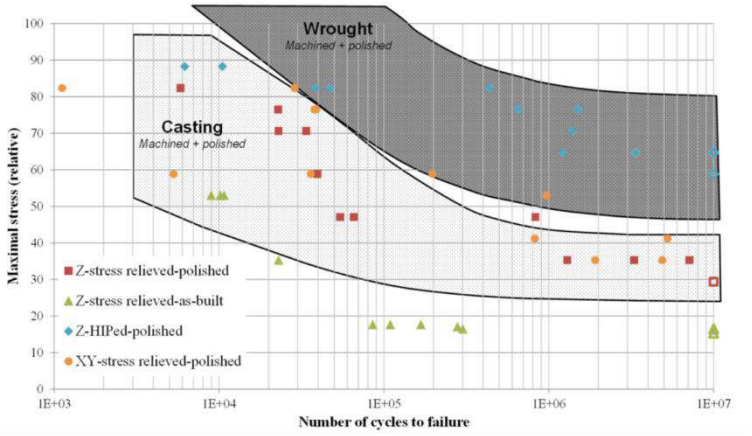

Figure 23: Fatigue behaviour of alloy Ti6-4 after stress relieving heat treatment and HIP compared to casted and wrought specimens [15]

Stress relieved specimens present a fatigue behaviour comparable to the one obtained for casted alloy Ti6-4. However, dispersion of the results have to be noticed, for example for tests performed at 60% of the maximum stress. After HIPing, the fatigue behaviour is similar to the one obtained for wrought alloy Ti6-4. Fracture surface analysis revealed that the failure of specimens start from defects present under the surface of the specimens.

To evaluate the effect of pores on mechanical properties, it is interesting to focus on specimens with the same microstructure but with and without pores. This approach has been led in Metaltechnics IRT project [16]. In this study, a first batch of specimens has been submitted to HIP treatment at 920°C – 1000 bar for 2 hours and a second batch has been submitted to a Simulated HIP (S-HIP) treatment, consisting of the application of the same thermal cycle but without applied pressure. The effort has been put on the cooling rate, as HIP vessel cannot perform cooling with high cooling rates. The duplication of microstructure being confirmed, tensile and fatigue tests have been performed. Results are presented in Figure 24 and Figure 25, respectively.

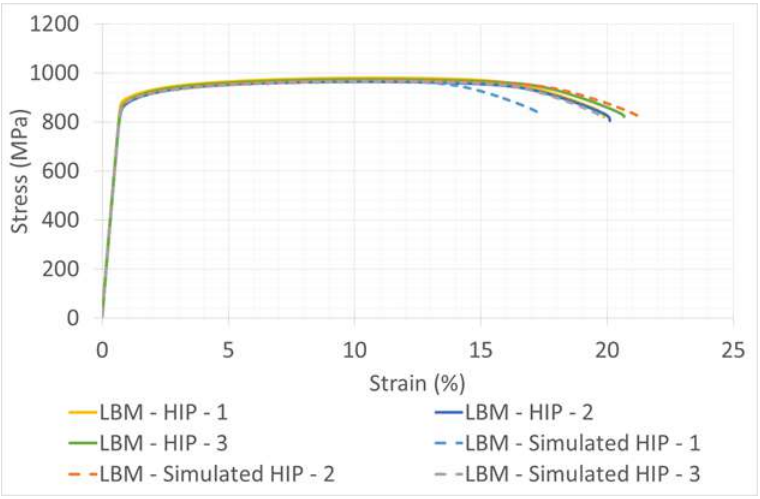

Figure 24: Tensile behaviour of LBM specimens after HIP and Simulated HIP [16]

Tensile strengths are equivalent between specimens submitted to HIP and S-HIP treatments. This result confirms that microstructures are equivalent between both treatments. The effect of pores is observed on the elongation to fracture. For HIP specimens, its dispersion is very low, results being very close to 20%. The absence of pressure during heat treatment brings a dispersion of results. Presence of pores is related to

this difference of behaviour, even if observation of fracture surfaces do not reveal any difference, ductile behaviour of the fracture being highlighted.

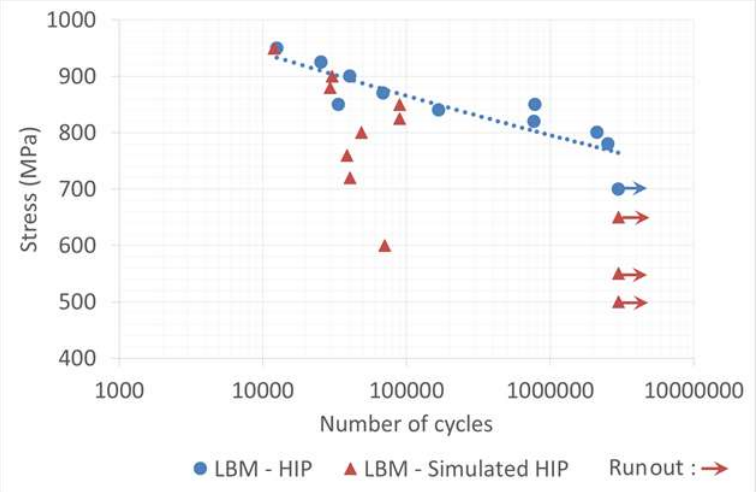

Figure 25: Fatigue behaviour of LBM specimens after HIP and Simulated HIP [16]

Fatigue behaviour of HIPed specimens is comparable to what is measured for wrought alloy, as discussed earlier. It can be fitted by a power law, $\sigma = kN^{\varepsilon}$, which is usually used for conventional alloy. For S-HIP specimens, fatigue behaviour at high stresses remain close to the one of HIPed specimens. Nevertheless, as the applied stress decreases, the number of cycles to failure decreases and an important dispersion of these values is measured. No clear tendency of the fatigue behaviour can be drawn. Observation of fracture surface of HIP specimens reveals that initiation of failure starts at the corner of the specimen, Figure 26 a), point of stress concentration.

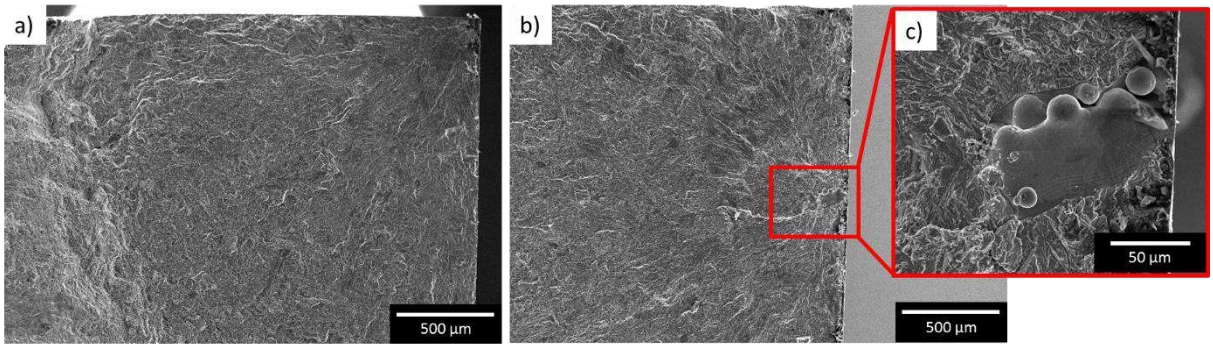

Figure 26: Exemples of fracture surfaces a) of HIPed specimen and b) & c) S-HIPed specimen [16]

On the contrary, observation of fracture surface of S-HIPed specimens reveals that failure is initiated on a defect situated near the surface, Figure 26 b). Observation of this zone at a higher magnification reveals the presence of an unmelted zone of about 100 x 70 µm. Failure of fatigue specimens is directly related to the presence of pores. Pores formation remaining a stochastic phenomenon, differences of mechanical behaviour between two specimens can be important, explaining results dispersion.

Summary

After LBM process, alloy Ti6-4 is composed of a full martensitic microstructure. The first aim of heat treatment is to manage this phase. Annealing at temperature from 600°C allows the decomposition of the phase and in consequence, stress relieving. Nevertheless, it is reported that the full decomposition is starting between 720°C and 800°C, depending on the author. By approaching β transus, formation of β phase is promoting. The final microstructure is, in consequence, dependent on the cooling rate. Martensite decomposition and formation of (α+β) microstructure induce a lowering of the tensile strength, but an increase of the ductility, compared to as built material. Heat treatment performed at temperature higher than β transus leads to the transformation of the microstructure into an equiaxed one. Final microstructure is dependent on the cooling from this high temperature and the subsequent annealing. Nevertheless, mechanical properties measured with these different microstructures are deeply linked with the presence of pores.

HIP treatment is usually performed into (α+β) domain and allows the closure of pores. It consequently improves the fatigue behaviour of the alloy.

2.2 Alloy Ti6-4 and EBM

EBM process is characterized by a pre-heating step in the process in order to sinter the powder to evacuate the electrical charges. In consequence, the powder bed is kept at quite high temperature during all the manufacturing. In the case of alloy Ti6-4, the temperature is set at 700°C, allowing the relieving of residual stresses. This is changing the solidification conditions leading to a different microstructure. Due to high cooling rate, columnar β grains are still forming. But, instead of being fully martensitic, the microstructure is composed of α lamellae surrounded by β phase. More details about this microstructures is provided in the project deliverable LIV-M-031-L1-409.

As the initial state is different from the one obtained after LBM, heat treatments performed are quite different. The manufacturing temperature being high, the microstructure is not composed of α' martensite. Heat temperature performed at lower temperature than the manufacturing temperature will have a slight influence on the microstructure.

2.2.1 Evolution of microstructure

(a) Sub-transus treatment

A study performed by Galarraga [17] is focused on the evolution of the microstructure after heat treatments performed at 600, 700 and 800°C. The evolution of α laths thickness is reported in Figure 27. After manufacturing, α lath thickness has been measured at 0.66 µm.

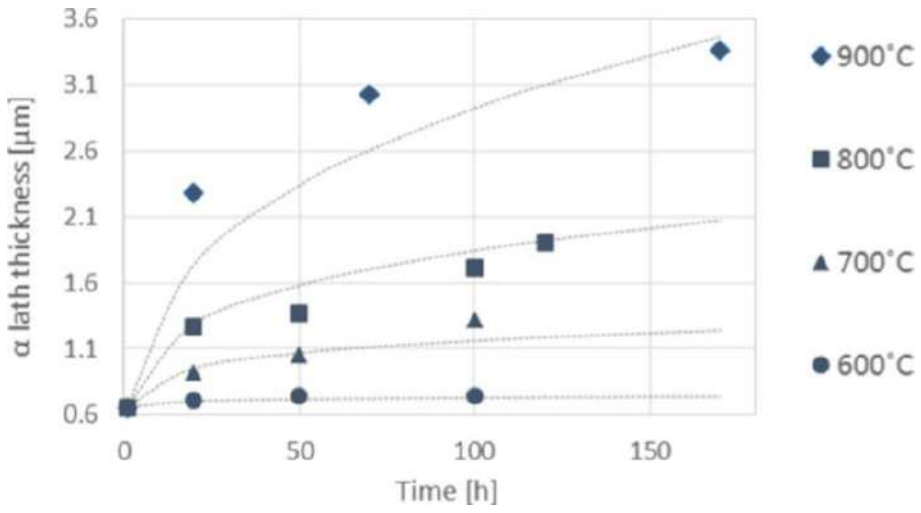

Figure 27: Evolution of α lath thickness after heat treatments at 600, 700 and 800°C until 120 hours [17]

Treatments performed at 600°C even for 100 hours did not lead to a significant evolution of the microstructure. Laths thickness after 100 hours of treatment is about 0.75 µm. The evolution of α laths is more pronounced after heat treatments at 700°C. After 100 hours of heat treatment, laths thickness almost doubled, reaching the size of about 1.3 µm. An increase of the temperature at 800°C leads to a faster growth of the laths thickness, reaching about 1.7 µm after 100 hours. Heat treatments at 900°C leads to a coarser microstructure. Nevertheless, microstructures of all these samples retain the columnar prior β grains.

The evolution of mechanical properties has been measured and reported as a function of the lath thickness. Hardness evolution and tensile properties are reported in Figure 28 and Figure 29, respectively.

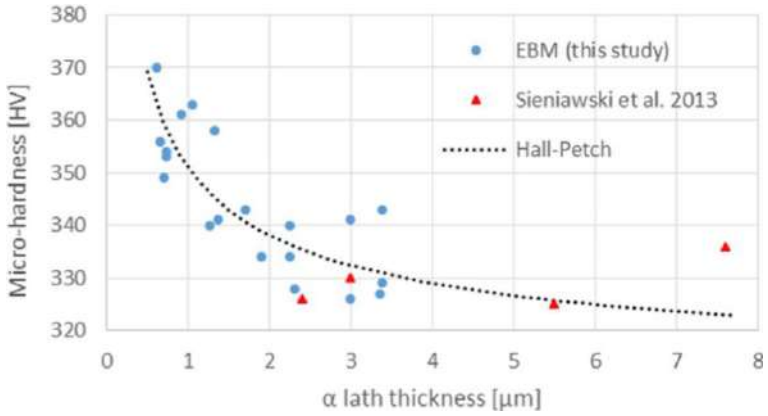

Figure 28: Evolution of micro-hardness as a function of α lath thickness [17]

As expected, as α laths thickness increases, the strength of the alloy decreases. The evolution of the hardness has been compared to the one calculated from the Hall-Petch relationship, Figure 28. Experimental results are in accordance with this evolution.

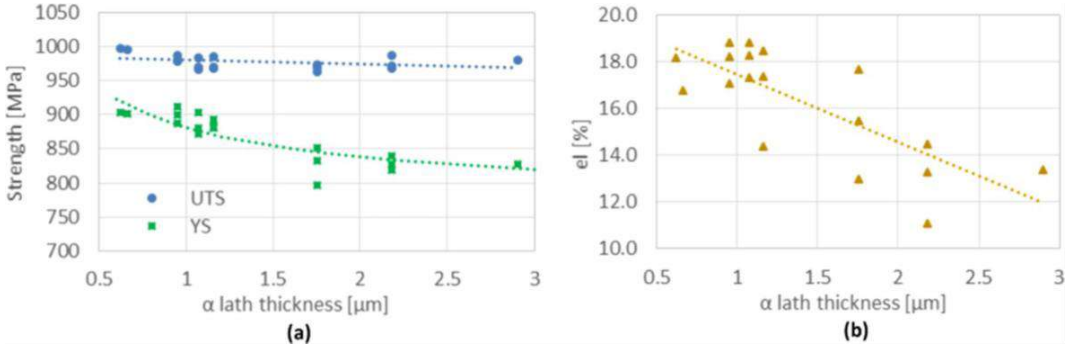

Figure 29: Evolution of a) tensile strength and b) elongation to failure as a function of the lath thickness [17]

Increase of α laths thickness did not lead to a huge modification of values of Ultimate Tensile Strength. Nevertheless, Yield Strength is largely affected, as it continuously decreases with the increase of laths thickness. Galarraga explains these results by the reduction of the effective slip length with the refinement of the microstructure, leading to the increase measured. As the microstructure is coarsening, the elongation to fracture is decreasing. The fact that transcrystalline mode of fracture has only been considered operational for α laths thickness range explains these results.

De Formanoir [18] performed heat treatments at 950°C on EBM alloy Ti6-4 with two cooling rates, air cooling and furnace cooling. Resultant microstructures are presented in Figure 30. Columnar former β grains are still observed after these two treatments, as α phase at the grain boundaries remains stable during heat treatment, retaining β grains. Nevertheless, some differences have to be outlined depending on the cooling rate. Furnace cooling leads to a coarsening of the microstructure, *i.e.* lamellae. During heat treatment at this temperature, diffusion of β stabilizing elements to the β phase is happening, promoting its growth. Moreover, cooling rate is largely influencing the presence of β phase.

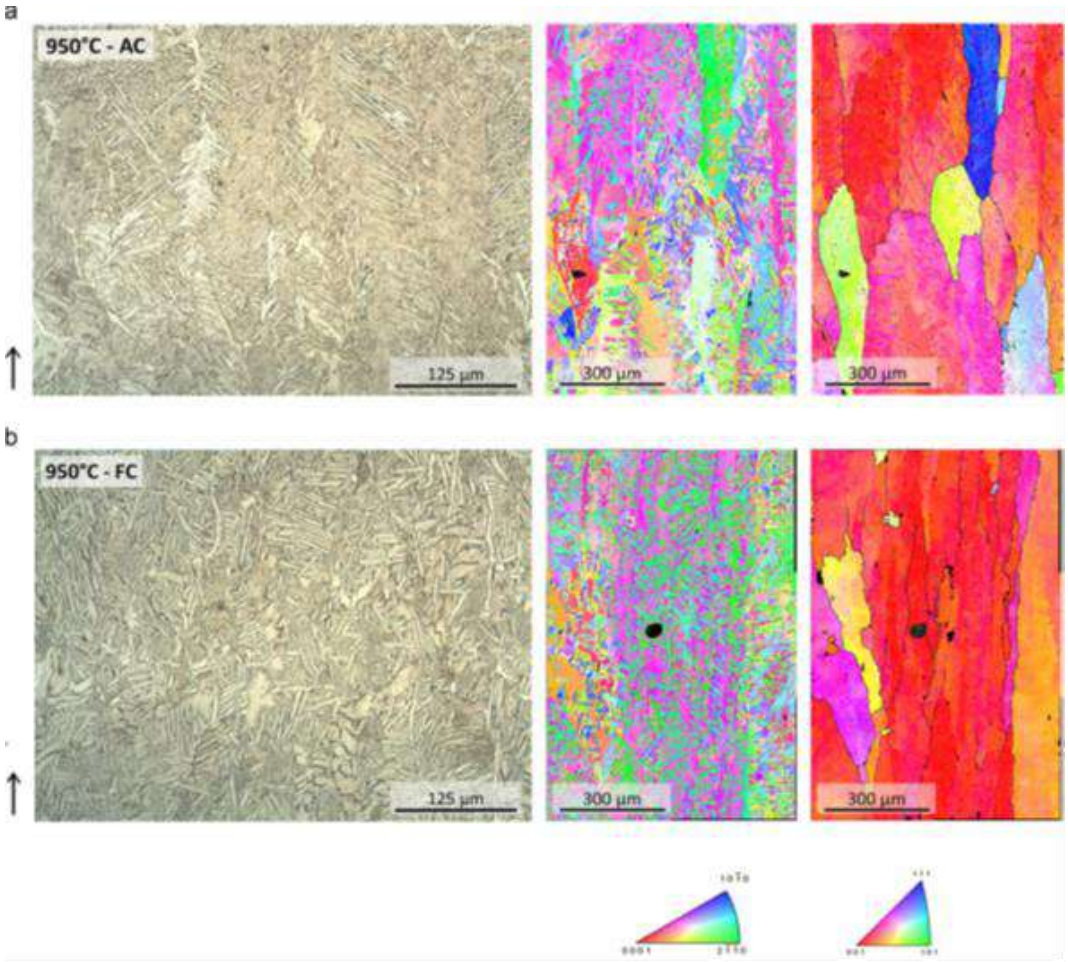

Figure 30: Microstructure of EBM alloy Ti6-4 after heat treatment of 1 h at 950°C followed by a) air cooling AC and b) furnace cooling [18]

As seen in Figure 31, β phase fraction is more important in the case of furnace cooling. The diffusion of β stabilizing elements is continuing during furnace cooling, promoting the growth of already formed β phase during EBM. It is considered in this study that air cooling is sufficiently quick to quench the alloy. Thus, no formation of β phase is occurring during cooling.

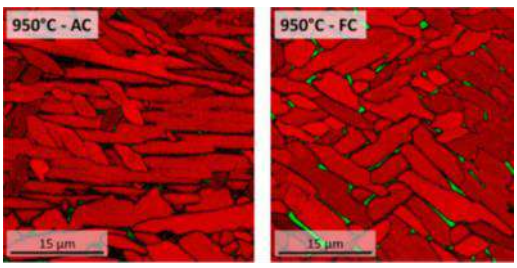

Figure 31: Phase distribution after heat treatments measured by EBSD. α in red and β in green [18]

Galarraga focused too on heat treatments performed in (α+β) domain, followed by two different cooling rates, water cooling and air cooling, and an annealing step at 450°C for 4 hours. Cycle description and resultant results are described in Figure 32.

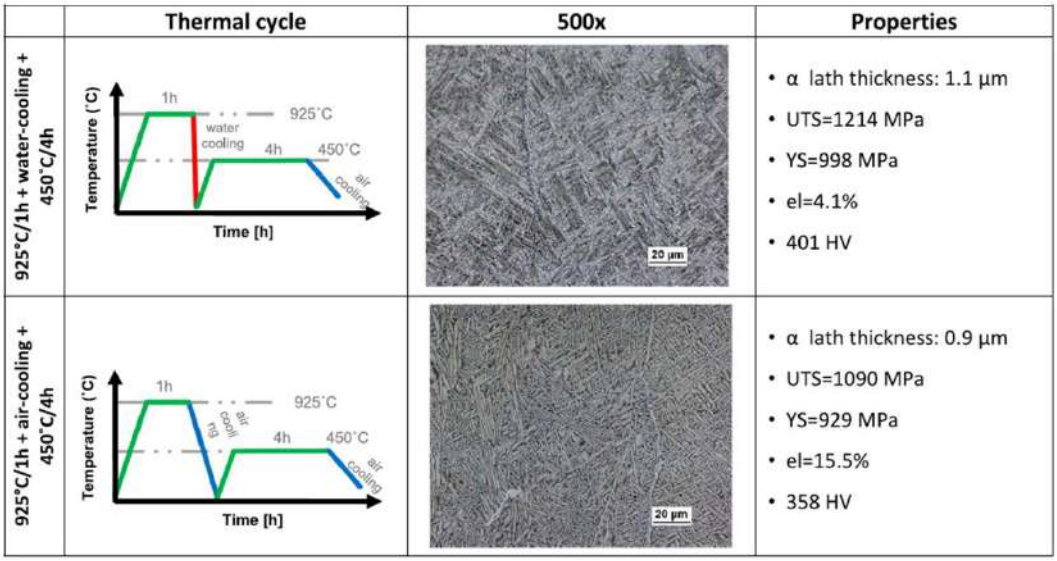

Figure 32: Thermal cycles, evolution of microstructure and mechanical properties [17]

Water cooling leads to the formation of martensite, as acicular phases are observed. Annealing at 450°C did not lead to its transformation into α phase. The presence of this phase explains the high strength and low elongation to fracture of the alloy after water cooling compared to air cooling. With this treatment, an increase of 0.3 µm of α lath thickness is measured.

Galarraga studied the effect of the annealing conditions after a solution heat treatment of 1 hour at 925°C followed by a water quench. Results of tensile tests are presented in *Figure* 33.

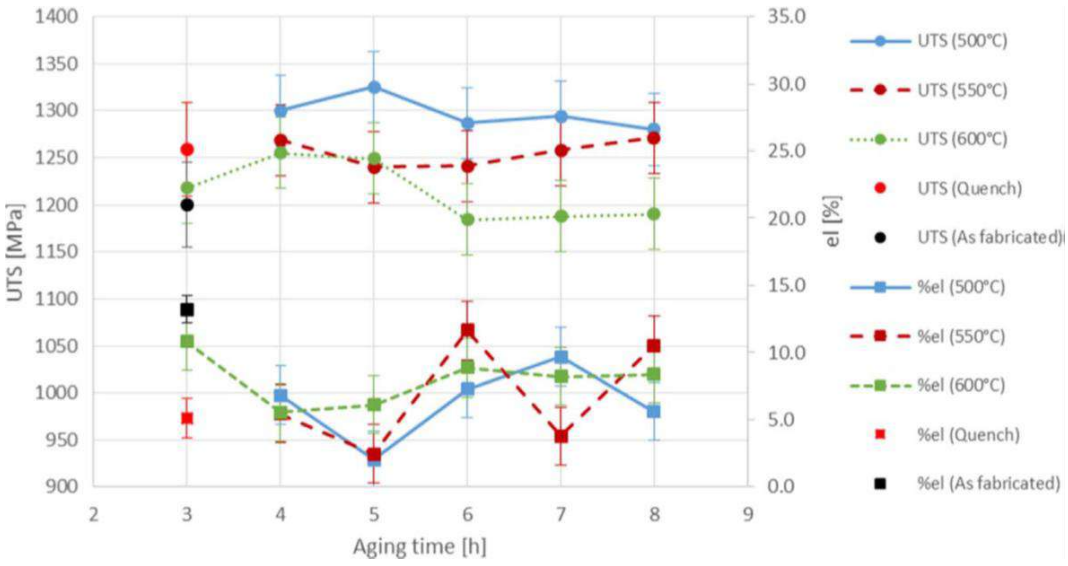

Figure 33: Evolution of tensile mechanical properties after different annealing conditions [17]

Modification of the mechanical behaviour can be achieved by changing annealing conditions. Nevertheless, even if high values of strength are reached, elongation to fracture values remain lower than 10%. These values are not in accordance with mechanical properties expected for a titanium alloy used for structural parts.

(b) Super-transus treatment

As for LBM, heat treatments above β transus temperature can be performed. As suggested by the CCT diagram in Figure 2, the cooling rate is of first importance when heat treating at this range of temperature. An example of the effect of cooling rate on the microstructure and mechanical properties is presented in Figure 34.

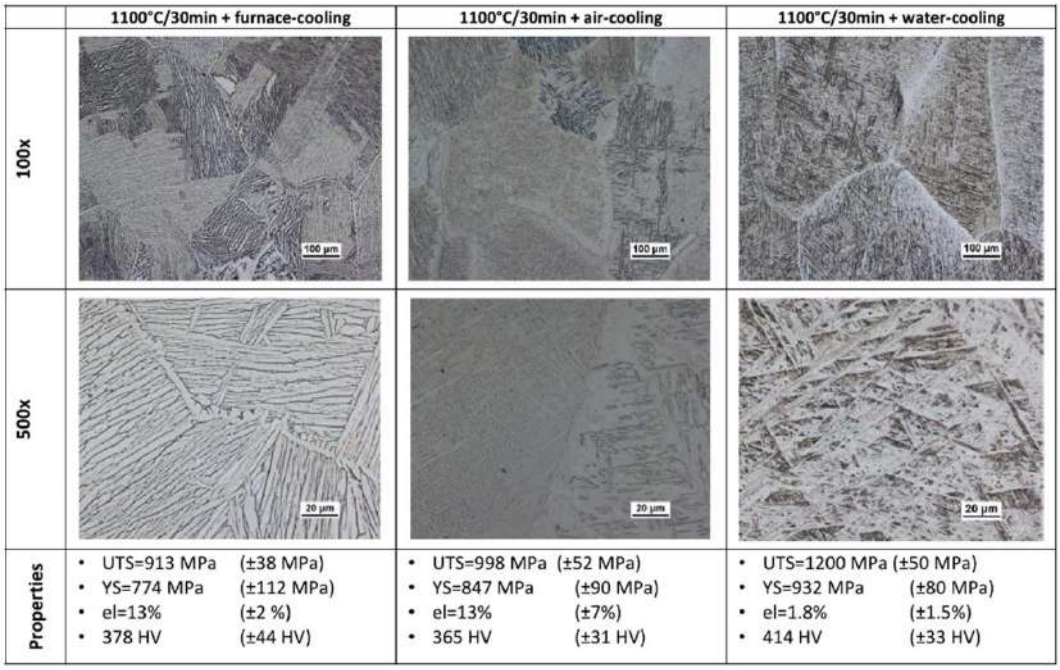

Figure 34: Effect of cooling rate after heat treatment at 1100°c for 30 minutes on microstructure and associated mechanical properties [17]

Galarraga [17] performed heat treatments at 1100°C for 30 min, insuring a complete transformation of the alloy in β phase, followed by three different cooling rates: furnace-cooling, air-cooling and water-cooling. Cooling rates have been measured and reported on a CCT diagram, Figure 35.

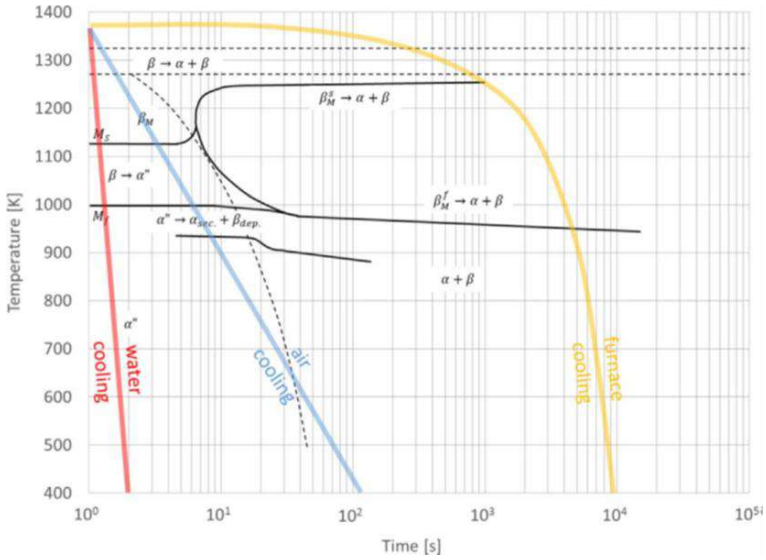

Figure 35: Furnace, air and water coolings reported on a CCT diagram [17]

In all cases, because of residence time at high temperature, the columnar structure of β grains has disappeared, the microstructure is equiaxed. After furnace cooling, the slowest cooling rate, a (α+β) lamellar microstructure is formed and is significantly coarser than the as built material. After air cooling, the (α+β)

lamellar microstructure is finer. According to Figure 35, cooling rate reached allows the formation of α' martensite which is partially decomposed during the end of cooling. Water cooling promotes the formation of a fully martensitic microstructure, as the cooling rate is sufficiently high. Thin laths are observed in Figure 34.

Evolution of mechanical properties in the different states are summarised into Figure 36. In this figure, equiaxed α+β stand for furnace cooling, columnar α+β for as built alloy, partially α' for air cooling and fully α' for water cooling.

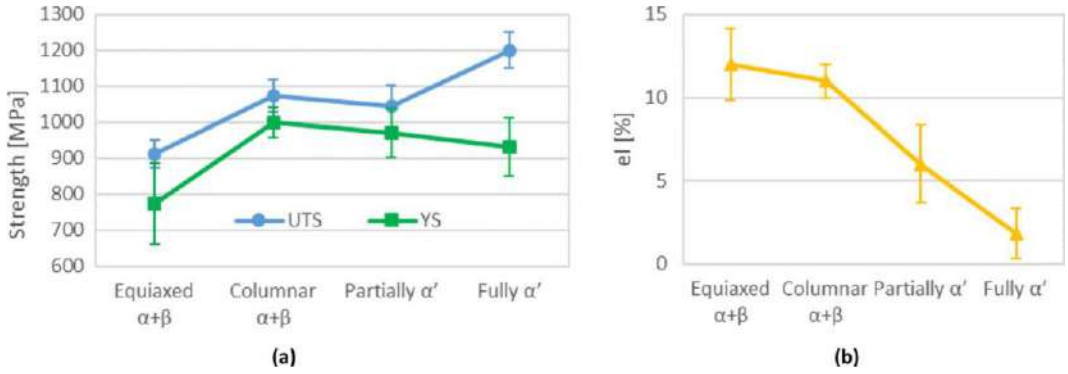

Figure 36: Evolution of tensile strengths and elongation to failure depending on the heat treatment conditions [17]

Because of the coarsening of the microstructure after super transus treatment and furnace cooling, tensile strengths are lower than as built alloy. Nevertheless, elongation to fracture has slightly increased even though an increase in the dispersion of the values has to be noted. As the fraction of martensite increases, tensile strengths increase too. A slight decrease of the yield strength is measured, but not explained by the authors. As expected, the elongation to fracture decreases because of the presence of the brittle martensite.

De Formanoir has done similar heat treatments [18]. The alloy has been heat heated up to 1040°C for 30 min and then submitted to air cooling and furnace cooling. As in the previous case described, furnace cooling leads to a coarser microstructure. In addition, EBSD analysis revealed that structure of the lamellae is quite different. As seen in Figure 37, air cooling leads to the formation of a Widmanstätten type microstructure, while furnace cooling induces a α colony microstructure. During cooling, α phase is forming at β grains boundaries. However, at lower cooling rates, α phase is nucleating from α phase present at grain boundaries into parallel plates, leading to the formation of colonies.

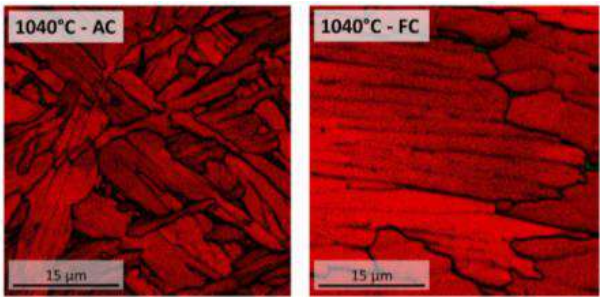

Figure 37: Evolution of lamellae morphology depending on the cooling rate [18]

Tensile tests have been performed afterwards. As expected, furnace cooling leads to lower tensile strengths, as the microstructures is coarser. But, the evolution of the fracture surface is interesting and reported in Figure 38. After air cooling, the fracture is occurring preferentially along the needle-like α lamellae, revealed by the sharpness of the fracture surface. After furnace cooling, presence of dimples reveal the more ductile failure mechanism.

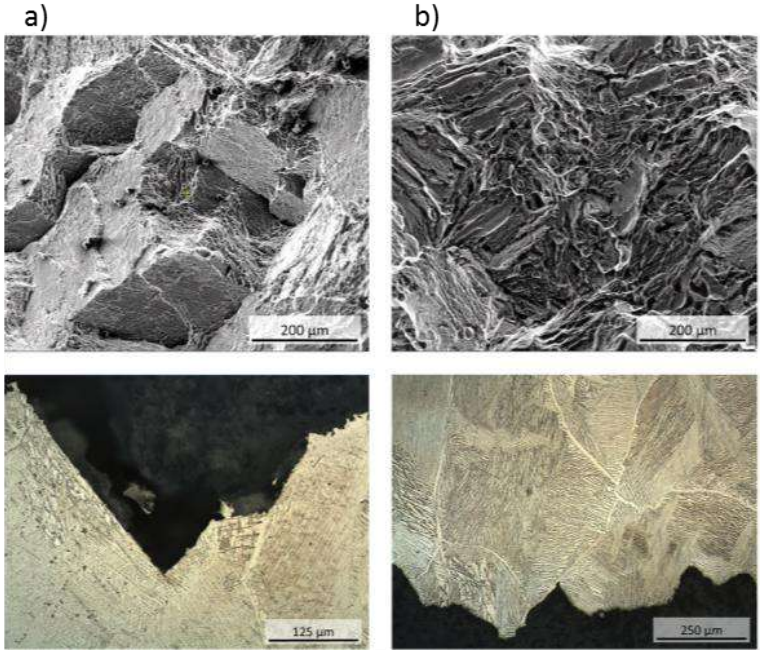

Figure 38: Fracture surface of specimens after heat treatment at 1040°C/30min followed by a) air cooling and b) furnace cooling [18]

(c) Hot Isostatic Pressure

One of the principal problem in powder bed additive manufacturing is the presence of pores. These pores lead to stress concentrations and potential premature failures. This effect is quite intensified in EBM, as pores size is greater than in LBM. An example of pores distribution is presented in Figure 39 a).

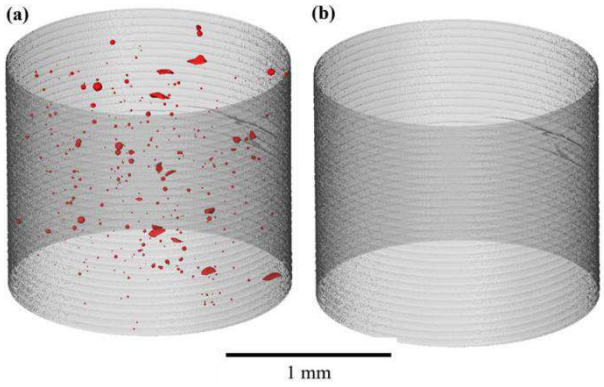

Figure 39: CT scans of the same cylinder a) in as built conditions and b) after HIP at 920°C and 1000 bar for 2 hours [19]

As in LBM process, HIP treatment is usually used to ensure the closure of the pores. Same parameters are used, *i.e.* 920°C, 1000 bar and 2 hours. The effect of this cycle is reported in Figure 39 b). No more pore is observed. The HIP treatment seems to totally erase the porosity. The effect on the microstructure is reported into Figure 40. The fact that heat treatment is occurring into (α+β) domain leads to the coarsening of α lamellae.

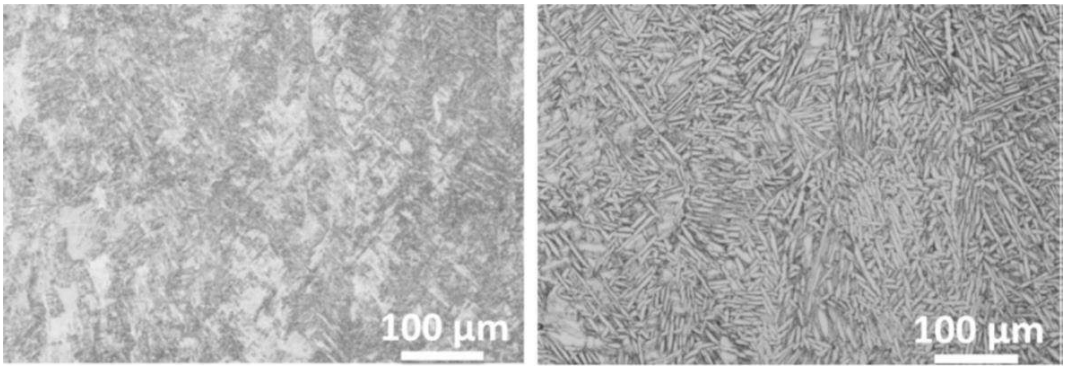

Figure 40: Microstructure of a) as built EBM sample and b) after HIP [20]

A more detailed view of the microstructure is proposed in Figure 41.

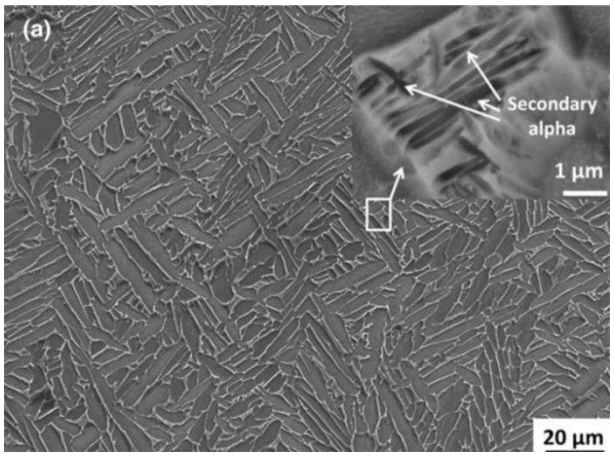

Figure 41: Focus on the microstructure after HIP of EBM specimen [20]

α phase lamellae, in dark into the picture, surrounded by β phase, in white, is observed. In some areas, a slight contrast is observed. Observation at higher magnification reveals the presence of secondary α, *i.e.* α phase coming from the transformation of β phase during cooling down.

The evolution of mechanical properties is reported in Figure 42. As the microstructure is coarsening, tensile strengths are lowering, whereas an increase of ductility, elongation and reduction of area, is measured. Moreover, in his papers, Lu worked on the homogeneity of the mechanical properties in the height of a sample. As observed in Figure 42, some differences are noticeable in as built specimens. After HIP, the tendency is to have a more homogeneous material.

Sample Status	Sample Positions	Yield Strength (MPa)	Ultimate Tensile Strength (MPa)	Elongation (Pct)	Reduction of Area (Pct)
As-built	top	903.6 ± 24.6	991.8 ± 21.7	16.4 ± 0.8	51.4 ± 2.4
	middle	928.7 ± 13.3	1011.7 ± 14.8	13.6 ± 1.4	38.9 ± 2.8
	bottom	911.9 ± 34.3	995.5 ± 28.5	13.5 ± 0.4	33.9 ± 1.5
HIP	top	800.1 ± 12.1	909.4 ± 2.4	16.7 ± 0.8	55.8 ± 3.0
	middle	813.3 ± 14.3	908.8 ± 3.2	17.7 ± 0.9	52.0 ± 1.9
	bottom	813.9 ± 16.2	910.6 ± 4.2	16.6 ± 0.8	51.9 ± 2.5
Standard	ASTM F3001-14	795.0	860.0	10.0	25.0

Figure 42: Evolution of mechanical properties after HIP [20]

The effect of HIP on the fatigue behaviour is important, as seen in Figure 43. The closure of pores leads to the increase of the fatigue properties. The difference of behaviour is more pronounced for high cycle fatigue. After HIP and on machined specimens, fatigue behaviour is comparable to the one of conventional alloy. The effect of surface roughness is of much importance considering the fatigue behaviour too.

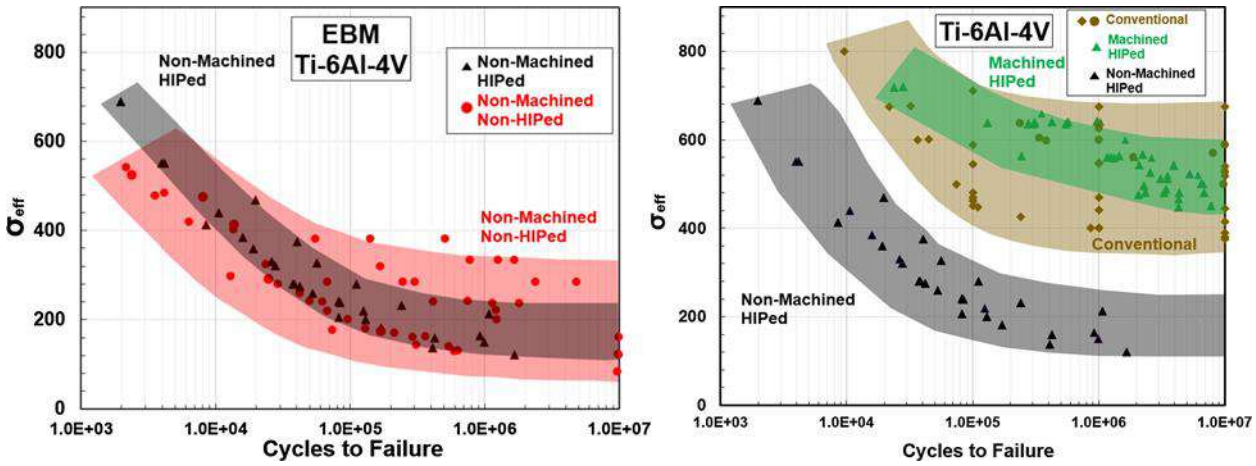

Figure 43: Fatigue behaviour of EBM alloy Ti6-4 after HIP on machined and non-machined specimens compared to conventional alloy [21]

As in the of LBM process, HIP and Simulated HIP treatments have performed on specimens built by EBM in Metaltechnics project [16]. Microstructure after HIP has been reproduced and tensile and fatigue tests have been performed. Results are presented in Figure 44 and Figure 46.

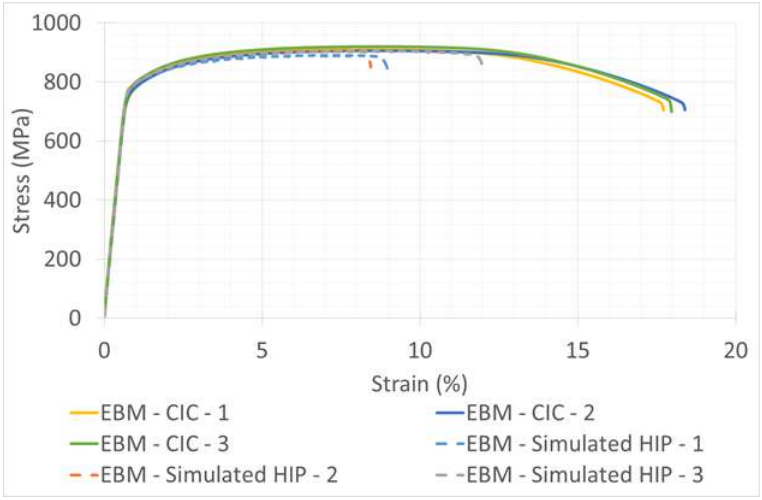

Figure 44: Tensile behaviour of EBM specimens after HIP and Simulated HIP [16]

Tensile strengths are equivalent between specimens submitted to HIP and S-HIP treatments. This result confirms that microstructures are equivalent between both treatments. Nevertheless, if HIPed specimens reveal an elongation to fracture of about 18 %, it is almost divided by two in the case of S-HIP specimens. It is interesting to notice that, in this case, as soon as that ultimate tensile strength is reached, failure is occurring. Observation of fracture surfaces reveals the ductile behaviour of the fracture after HIP. After S-HIP, the lack of deformation is observed as the fracture surface remains rectangular. Moreover, zones without deformation are revealed, these zones being composed of unmelted powder, Figure 45. The failure is directly linked with pores presence.

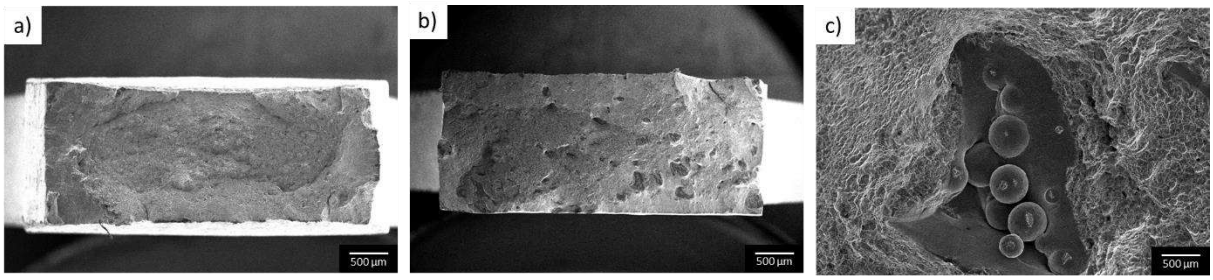

Figure 45: Fracture surfaces of tensile specimens after a) HIP and b) & c) S-HIP [16]

Fatigue behaviour is largely affected by the absence of pressure during heat treatment. Even if behaviours remain close at high stress fatigue, fatigue behaviour is largely reduced for S-HIPed specimens compared to HIPed ones. Endurance limit can be estimated to about 150 MPa for S-HIP compared to about 650 MPa after HIP. But, on the contrary to LBM, the dispersion of results is low, results can be fitted by an usual power law. This tends to indicate that the distribution of pores is homogeneous in the part and that an elementary representative volume has been solicited during these fatigue tests.

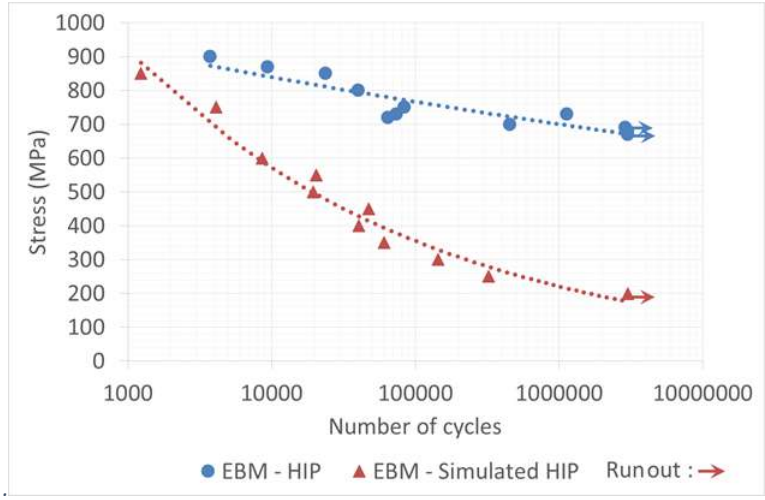

Figure 46: Fatigue behaviour of EBM specimens after HIP and Simulated HIP [16]

Fracture surface observation of S-HIPed specimens reveals, as in the case of tensile tests, the initiation of failure on unmelted zones, Figure 47.

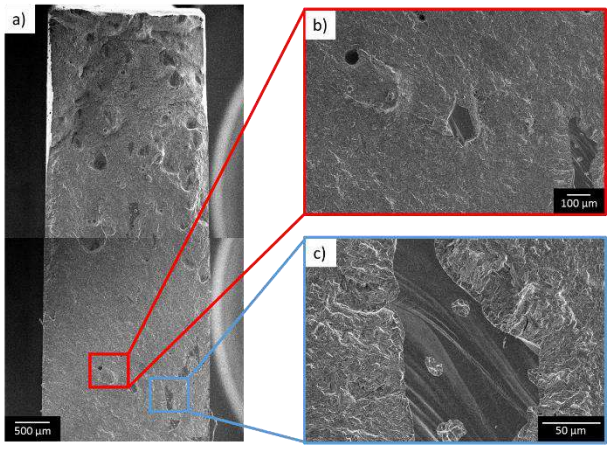

Figure 47: Fracture surfaces of fatigue specimen after S-HIP [16]

De Formanoir [22] studied the effect of heat treatment after HIP. The goal of her study was to increase the workability of the alloy through heat treatment. For this, she used a quite different approach. After performing HIP, specimens were heat treated from 850°C to 980°C for 2 hours and water quench. The evolution of microstructure is reported in Figure 48.

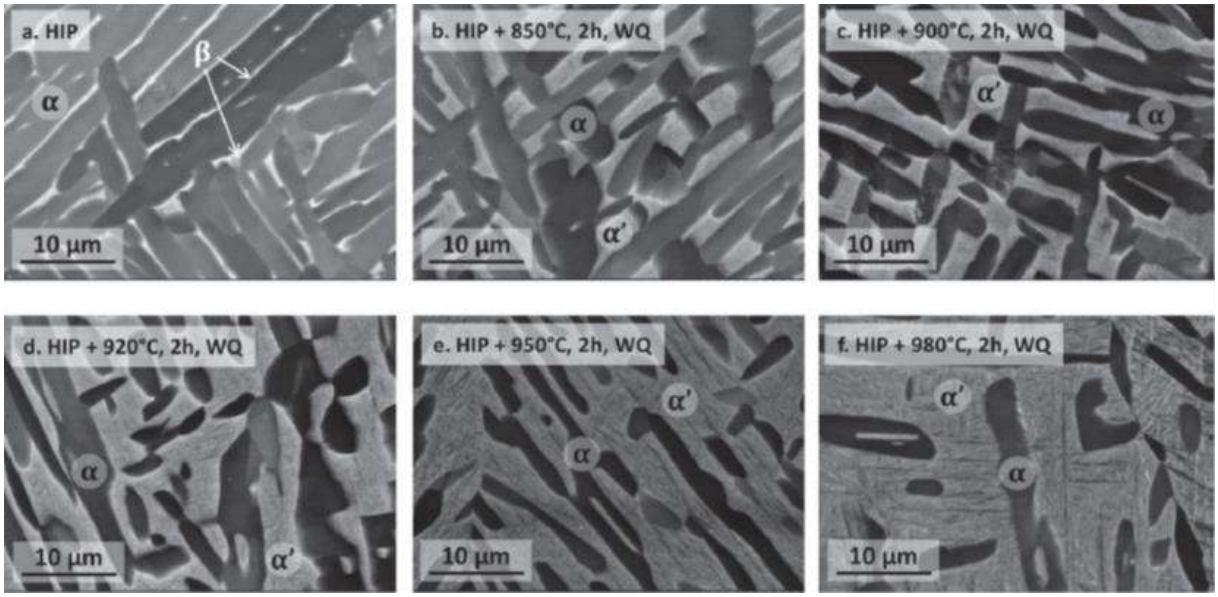

Figure 48: Evolution of microstructure after HIP followed by annealing at different temperatures and a water quench [22]

Because of the water quench, β phase present at high temperature during annealing is transforming into α' martensite. The fraction of martensite is increasing with the annealing temperature. This is related to the fact that as the temperature is closer to β transus point, the fraction of β phase is increasing. Mechanical properties of these different microstructures have been evaluated by tensile tests, Figure 49. It has be noted that true stress and strain are used in this case.

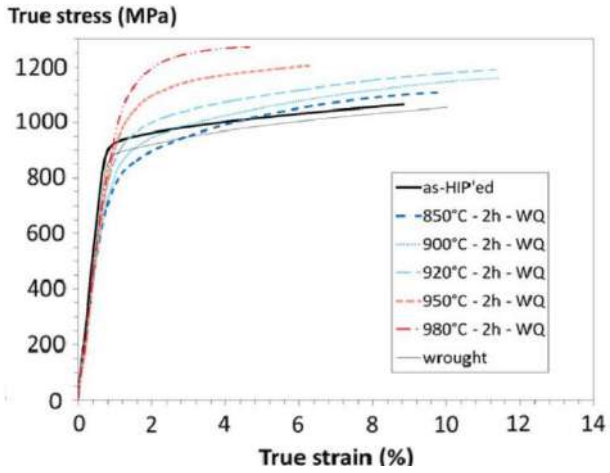

Figure 49: Evolution of mechanical properties after different heat treatments [22]

Results show that with a small amount of martensite, Yield Strength is lower than after HIP, maybe because of the presence of soft orthorhombic martensite, but, Ultimate Tensile Strength is increasing. As the annealing temperature increases and so the fraction of martensite, Yield Strength and Ultimate Tensile Strength are increasing. But the difference between them tend to decrease. The approach developed in this paper which is to create a material by mixing a hard material, α' martensite, with a soft one, α phase, is similar to the one that lead to the creation of Dual-Phase steels. The difference of mechanical behaviour between the phases leads to the creation of numerous geometrically necessary dislocations to accommodate the difference of strain between them. As a consequence, work-hardening of these materials is good.

However, even if the tensile mechanical properties are interesting, it has to be outlined that the alloy is mainly composed of martensite. It would be interesting to focus on its role on the fatigue and toughness of the alloy.

Nevertheless, in the introduction of this document, it has been discussed that after HIP, swelling of pores can happen during subsequent heat treatment. This aspect is not well documented on additively manufactured parts, exception of the work from Tammas-Williams [19]. In this paper, closure and reopening of pores have been carefully followed by the use of CT scans. In this study, argon gas atomised powder has been used. As EBM process is occurring under helium dynamic vacuum, pores related to the presence of argon cited in this article come from entrapped gas into the powder. Results in as built state and after HIP have already been presented in Figure 39. CT scans performed on the same sample and location after different heat treatment at high temperature, 1035°C and 1200°C, are reported in Figure 50. The voxel size was set to 2 µm, leading to a reliable identification of an object of an equivalent diameter of 5.2 µm.

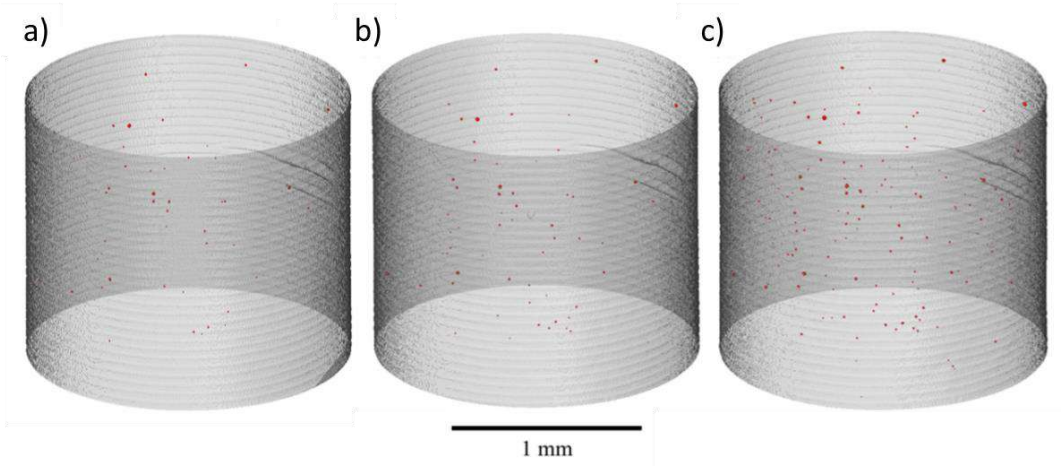

Figure 50: Results of CT scans after heat treatment at a) 1035°C for 10 min, b) 1035°C for 10 h and c) 1200°C for 10 min [19]

When comparing these results with the one obtained after HIP, it can be seen that pores are effectively appearing after subsequent heat treatments. The quantification data of pores presence is reported in Figure 51.

Condition	Volume fraction (%)	Number	Mean equiv. dia. (µm)	Max. equiv. dia. (µm)
As-built	0.0397	309	13.3	53.3
HIPed	0.0000	0	–	–
HT1	0.0007	49	8.4	18.6
HT2	0.0011	63	9.2	20.0
HT3	0.0026	140	9.4	21.6

Figure 51: Quantification data on the pores presence after different heat treatments [19]

These data confirm the disappearance of all pores after HIP. After heat treatment at 1035°C for 10 minutes, 49 pores have appeared with a mean equivalent diameter of 8.4 µm. Heat treating at this temperature up to 2 hours leads to a slight increase of the number of pores but a more significant increase of the mean equivalent diameter. By increasing the temperature up to 1200°C, the number of pores has reached 140, more than two times the number of pores present after heat treatment at 1035°C for 2 hours. It has be noted that the mean equivalent diameter remains stable between these two heat treatments. An example of the evolution of one pore after the different heat treatments is reported in Figure 52.

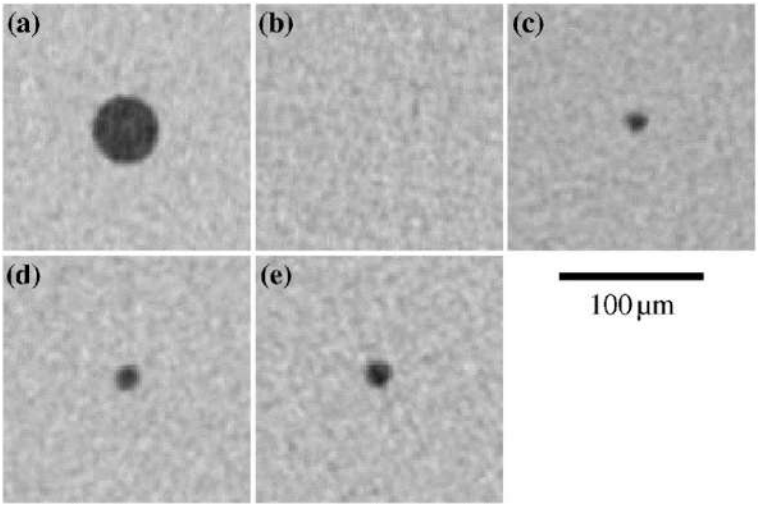

Figure 52: Example of the evolution of a pore a) in as built conditions, b) after HIP, c) after 1035°C for 10 min, d) after 1035°C for 2 hours and e) after 1200°c for 10 min [19]

In addition to these data, Tammas-Williams get interested in two other aspects: the aspect ratio and the equivalent diameter in as-built conditions compared to the one after heat treatment. These results are presented in Figure 53 and Figure 54, respectively.

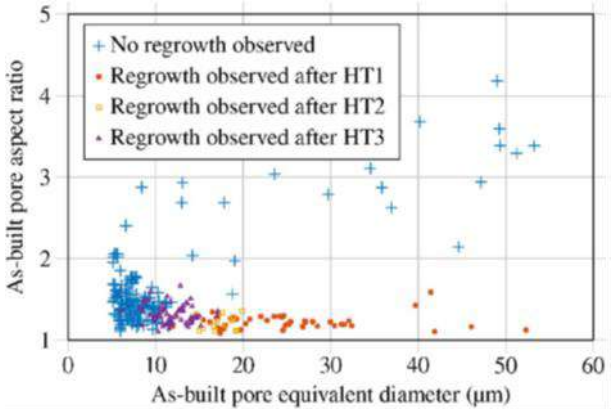

Figure 53: Evolution of aspect ratio and equivalent diameter as a function of heat treatment applied [19]

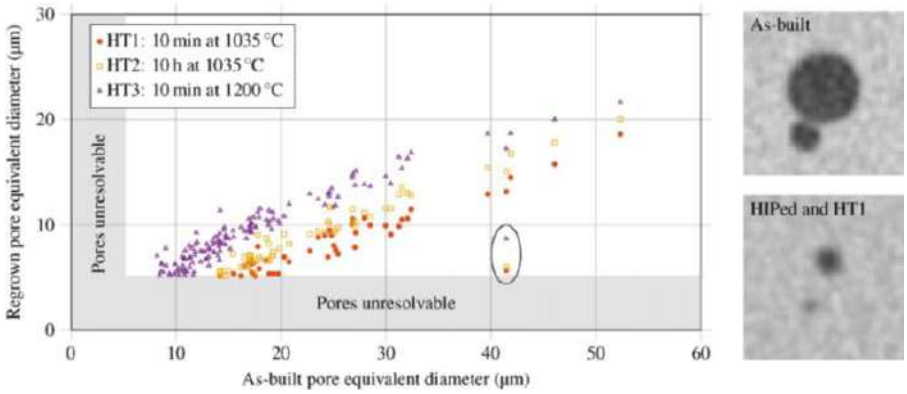

Figure 54: Evolution of pores size according to the different heat treatment steps [19]

Several conclusions can be made from these data. After HIP, lot of pores are not growing again during subsequent heat treatment, Figure 53. Pores present in the as-built condition can be divided in two categories. First, pores with a size lower than 10 µm. These pores present in majority an aspect lower than two and close to one, meaning that they are quite circular/ spherical. Second category is composed of pores with equivalent diameter higher than 10 µm. These pores present a high aspect ratio. All these pores have

been erased through HIP. After heat treatment, pores that reappear present, in majority, a size lower than 10 µm even if larger ones are observed too. But, they possess a low aspect ratio, close to one. This means that pores that are growing during heat treatment are quite circular. Thus, pores with high aspect ratio which are the more detrimental to mechanical properties seems to be erased by HIP and do not grow after subsequent heat treatment.

As explained earlier, high pressure and high temperature can lead to the dissolution of gas into the metal. Nevertheless, argon is not totally soluble into titanium and cannot escape the metal during HIP treatment. In consequence, argon remains into the material, into collapsed pores applying a high internal pressure on the material. In the absence of pressure during subsequent heat treatments, as the strength of the material has decreased, creep phenomenon can start, leading to the reformation of pores. Moreover, as the temperature increases, creep rate increases too, leading to more pores formation. The mechanical behaviour around a pore is quite complicated. As one pore is a closed system, it can be considered that the quantity of gas into it remains stable. But, as the pore grows, the internal pressure decreases, until reaching a mechanical equilibrium state. This equilibrium seems to be reached quite fast as data at 1035°C show that most of the pores regrowth happen in the first 10 minutes.

As mentioned in Figure 54, pores which are growing again during subsequent heat treatment present a size lower than the original pores. The increase of size for longer duration at a given temperature does not seem to be important. The increase of temperature induces a quite steep increase of pores size. A particular case is outlined in Figure 54. This case is just a measurement error. As shown, in as built conditions, the pore has been considered unique although it corresponds to the juxtaposition of two pores, as its morphology after heat treatment shows.

Summary

In the case of EBM, as the alloy is in a more stable state due to the fact that manufacturing occurs at high temperature, heat treatments do not have to deal with the management of martensite. The effect of heat treatments performed at temperature lower than β transus with a slow cooling is mainly the coarsening of the microstructure, and especially α lamellae. This coarsening induces a softening of the alloy. When cooling rate increases, formation of martensite can happen. In this case, an annealing at lower temperature can be performed. When heat treatment is performed above β transus, columnar grain structure inherited from the process is modified. An equiaxed microstructure is formed. Cooling rate from this temperature is of great importance, as (α+β) lamellar structure can be formed or a fully martensitic one.

HIP treatment induces the annihilation of porosity. Mechanical properties after HIP, especially in fatigue, are comparable to the one measured for conventional alloy. As suggested by Aktinson, porosity regrowth has been observed for heat treatment performed after HIP. This phenomena is induced by the high pressure into the pores and the creeping of the alloy at high temperature. Nevertheless, HIP is reducing the aspect ratio and the size of pores, *i.e.* their detrimental effect.

3 Conclusions

Heat treatment performed on alloy Ti6-4 elaborated by Powder Bed Fusion processes have different aims depending on the process. In the case of LBM, the management of martensite is one of the priority, for structural applications. In the case of EBM, as process is occurring at high temperature, microstructure is more compatible with this type of applications. Nevertheless, in both processes, management of the pores is of primary interest. Cracks are preferentially initiating from these sites, leading to premature failure of the material. HIP treatment is usually used to overcome this problem, which seems to eradicate porosity.

The evolution of the anisotropy of mechanical properties consecutive of heat treatments is not so much reported in the literature. Alloy Ti6-4 manufactured by PBF processes is reported to possess an anisotropic mechanical behaviour, as described in the IRT deliverable LIV-M-031-L1-409. The evolution of this anisotropy after heat treatment is of great interest for industrial applications.

One surprising point developed in several studies is the use of water quench after heat treatment. Particularity of titanium alloys is that α phase which is stable at room temperature is a hexagonal close packed lattice cell. This cell presents a high anisotropy of dilatation coefficient between its c axis and a & b axis. This leads to an inhomogeneous strain accommodation and consequently, to the formation of residual stresses. High cooling rate does not allow them to be relieved. This is happening by deformation of the part after quenching. This phenomenon is manageable for laboratory scale specimens but in the case of complex parts with the mix of thin and thick walls, high deformation of certain zones are expected.

Moreover, even if PBF processes induce high cooling rates to the material during the manufacturing, chemical segregation is observed, as seen in the case of alloy 718. This may be the same case in alloy Ti6-4 in as built samples too. The study of phase's formation during subsequent heat treatment can give data on these chemical segregations. Then, the effect of heat treatments on them is of primary interest in order to avoid formation of detrimental phases during parts life.

Another approach of heat treatments, not reported in the literature, can be not to close pores but to adapt the microstructure to the local stress concentrations brought. This approach has not been developed in the literature. Nevertheless, in some applications, this can be of great interest. Furthermore, HIP vessel actually used are limited in cooling rates performance. New vessels are able to reach cooling rates of several tens of degrees per second, as high pressure gas become a good heat exchanger. These new vessels open the door to full treatment realised under pressure, which may be beneficial at the end. Indeed, effect of pressure on phase transformation has been reported on steels leading to finer microstructure and stronger material. It will be interesting to determine it for other systems too.

Nevertheless, treatment sequence composed of HIP followed by a subsequent heat treatment raises the problem of pores regrowth. This phenomenon has been reported in one study on EBM process and not on LBM process. However, as LBM process is occurring under an over pressurization of Argon, the stability of pores formed is a question of great interest, as gas pressure into pores must reach high values during subsequent heat treatment or long term ageing.

From a global point of view, heat treatments actually performed on alloy elaborated by PBF processes are inspired from heat treatments performed on wrought or casted materials. The thickness of microstructure, explaining high mechanical properties in as built conditions, is unfortunately often erased. Elementary data, such as phase transformation diagram applied to these new initial states, are necessary to go further into the understanding and the optimisation of the heat treatment applied to additive manufacturing. An example of optimisation is present in the literature. A very fine (α+β) lamellar microstructure restrained to former α' martensite has been reported by Xu [23] on alloy Ti6-4 processed by LBM. This microstructure leads to a material with a combination of high strength and high ductility. This microstructure was first created by a parameter evolution during manufacturing but has been recreated after heat treatment at very low temperature. This example illustrates the need to get interest into deeper understanding of the phase evolution during heat treatment.

4 References

[1] H. V. Atkinson and S. Davies, “Fundamental aspects of hot isostatic pressing: An overview,” *Metallurgical and Materials Transactions A,* vol. 31, pp. 2981-3000, 12 2000.

[2] B. Y. Lyubov and V. G. Tsyganenko, “Theory of the effect of pressure on the decomposition process of austenite in the upper range of subcritical temperatures,” *Metal Science and Heat Treatment,* vol. 10, pp. 85-88, 2 1968.

[3] S. Mashl, A. Eklund and M. Ahlfors, "Rapid high pressure gas quenching during hip: Combining densification and heat treatment into a single process," Quintus Technologies AB, Quintusvägen 2, Västeras, SE-72166, Sweden, 2016.

[4] A. Angré, O. Karlsson and E. Claesson, "Phase transformation under isostatic pressure in HIP," Swerea KIMAB, Isafjordsgatan 28A, Kista, 164 40, Sweden, 2016.

[5] A. Angré, M. Ahlfors, D. Chasoglou, L. Larsson, E. Claesson and O. Karlsson, “Phase transformation under isostatic pressure in HIP,” *Powder Metallurgy,* vol. 60, pp. 167-174, 5 2017.

[6] T. Ahmed and H. J. Rack, “Phase transformations during cooling in α+β titanium alloys,” *Materials Science and Engineering: A,* vol. 243, pp. 206-211, 3 1998.

[7] C. Qiu, N. J. E. Adkins and M. M. Attallah, “Microstructure and tensile properties of selectively laser-melted and of HIPed laser-melted Tiâ€“6Alâ€“4V,” *Materials Science and Engineering: A,* vol. 578, pp. 230-239, 8 2013.

[8] T. Vilaro, C. Colin and J. D. Bartout, “As-Fabricated and Heat-Treated Microstructures of the Ti-6Al-4V Alloy Processed by Selective Laser Melting,” vol. 42, pp. 3190-3199--, 2011.

[9] B. Vrancken, L. Thijs, J.-P. Kruth and J. Van Humbeeck, “Heat treatment of Ti6Al4V produced by Selective Laser Melting: Microstructure and mechanical properties,” *Journal of Alloys and Compounds,* vol. 541, pp. 177-185, 11 2012.

[10] R. Pederson, O. Babushkin, F. Skystedt and R. Warren, “Use of high temperature X-ray diffractometry to study phase transitions and thermal expansion properties in Ti-6Al-4V,” *Materials Science and Technology,* vol. 19, pp. 1533-1538, 11 2003.

[11] L. Xu, R. Guo, C. Bai, J. Lei and R. Yang, “Effect of Hot Isostatic Pressing Conditions and Cooling Rate on Microstructure and Properties of Ti-6Al-4V Alloy from Atomized Powder,” *Journal of Materials Science & Technology,* vol. 30, pp. 1289-1295, 12 2014.

[12] M. Benedetti, M. Cazzolli, V. Fontanari and M. Leoni, “Fatigue limit of Ti6Al4V alloy produced by Selective Laser Sintering,” *Procedia Structural Integrity,* vol. 2, pp. 3158-3167, 2016.

[13] M.-W. Wu and P.-H. Lai, “The positive effect of hot isostatic pressing on improving the anisotropies of bending and impact properties in selective laser melted Ti-6Al-4V alloy,” *Materials Science and Engineering: A,* vol. 658, pp. 429-438, 3 2016.

[14] G. Kasperovich and J. Hausmann, “Improvement of fatigue resistance and ductility of TiAl6V4 processed by selective laser melting,” *Journal of Materials Processing Technology,* vol. 220, pp. 202-214, 6 2015.

[15] V. Chastand, A. Tezenas, Y. Cadoret, P. Quaegebeur, W. Maia and E. Charkaluk, “Fatigue characterization of Titanium Ti-6Al-4V samples produced by Additive Manufacturing,” *Procedia Structural Integrity,* vol. 2, pp. 3168-3176, 2016.

[16] J. Hugues, C. Larignon and S. Pérusin, “Post traitements sur l'alliage TA6V élaboré en fabrication Additive,” Rapport Projet Metaltechnics, 2017.

[17] H. Galarraga, R. J. Warren, D. A. Lados, R. R. Dehoff, M. M. Kirka and P. Nandwana, “Effects of heat treatments on microstructure and properties of Ti-6Al-4V ELI alloy fabricated by electron beam melting (EBM),” *Materials Science and Engineering: A,* vol. 685, pp. 417-428, 2 2017.

[18] C. Formanoir, S. Michotte, O. Rigo, L. Germain and S. Godet, “Electron beam melted Ti-6Al-4V: Microstructure, texture and mechanical behavior of the as-built and heat-treated material,” *Materials Science and Engineering: A,* vol. 652, pp. 105-119, 1 2016.

[19] S. Tammas-Williams, P. J. Withers, I. Todd and P. B. Prangnell, “Porosity regrowth during heat treatment of hot isostatically pressed additively manufactured titanium components,” *Scripta Materialia,* vol. 122, pp. 72-76, 9 2016.

[20] Y. Lu, H. B. Tang, Y. L. Fang, D. Liu and H. M. Wang, “Microstructure evolution of sub-critical annealed laser deposited Ti-6Al-4V alloy,” *Materials & Design,* vol. 37, pp. 56-63, 5 2012.

[21] A. H. Chern, P. Nandwana, T. Yuan, M. M. Kirka, R. R. Dehoff, P. K. Liaw and C. E. Duty, “A Review on the Fatigue Behavior of Ti-6Al-4V Fabricated by Electron Beam Melting Additive Manufacturing,” *International Journal of Fatigue,* 9 2018.

[22] C. Formanoir, A. Brulard, S. Vivès, G. Martin, F. Prima, S. Michotte, E. Rivière, A. Dolimont and S. Godet, “A strategy to improve the work-hardening behavior of Ti-6Al-4V parts produced by additive manufacturing,” *Materials Research Letters,* vol. 5, pp. 201-208, 5 2017.

[23] W. Xu, M. Brandt, S. Sun, J. Elambasseril, Q. Liu, K. Latham, K. Xia and M. Qian, “Additive manufacturing of strong and ductile Ti-6Al-4V by selective laser melting via in situ martensite decomposition,” *Acta Materialia,* vol. 85, pp. 74-84, 2 2015.

[24] H. Galarraga, D. A. Lados, R. R. Dehoff, M. M. Kirka and P. Nandwana, “Effects of the microstructure and porosity on properties of Ti-6Al-4V ELI alloy fabricated by electron beam melting (EBM),” *Additive Manufacturing,* vol. 10, pp. 47-57, 4 2016.

End of document